

1 **Examination of varying mixed-phase stratocumulus clouds in terms of their**  
2 **properties, ice processes and aerosol-cloud interactions between polar and**  
3 **midlatitude cases: An attempt to propose a microphysical factor to explain the**  
4 **variation**

5  
6 Seoung Soo Lee<sup>1,2,3</sup>, Chang-Hoon Jung<sup>4</sup>, Jinho Choi<sup>5</sup>, Young Jun Yoon<sup>6</sup>, Junshik Um<sup>5,7</sup>,  
7 Youtong Zheng<sup>8</sup>, Jianping Guo<sup>9</sup>, Manguttathil. G. Manoj<sup>10</sup>, Sang-Keun Song<sup>11</sup>

8  
9 <sup>1</sup>Science and Technology Corporation, Hampton, Virginia

10 <sup>2</sup>Earth System Science Interdisciplinary Center, University of Maryland, College Park,  
11 Maryland, USA

12 <sup>3</sup>Research Center for Climate Sciences, Pusan National University, Busan, Republic of  
13 Korea

14 <sup>4</sup>Department of Health Management, Kyungin Women's University, Incheon, Republic of  
15 Korea

16 <sup>5</sup>Department of Atmospheric Sciences, Pusan National University, Busan, Republic of  
17 Korea

18 <sup>6</sup>Korea Polar Research Institute, Incheon, Republic of Korea

19 <sup>7</sup>Institute of Environmental Studies, Pusan National University, Busan, Republic of Korea

20 <sup>8</sup>Department of Earth and Atmospheric Sciences, University of Houston, Houston, Texas,  
21 USA

22 <sup>9</sup>State Key Laboratory of Severe Weather, Chinese Academy of Meteorological Sciences,  
23 Beijing 100081, China

24 <sup>10</sup>Advanced Centre for Atmospheric Radar Research, Cochin University of Science and  
25 Technology, Kerala, India

26 <sup>11</sup>Department of Earth and Marine Sciences, Jeju National University, Jeju, Republic of  
27 Korea

28

29

30

31

32

33

34

35

36

37

38

39

40

41

42

43

44

45

46

47

48 Corresponding author: Seoung Soo Lee, Chang-Hoon Jung and Sang-Keun Song

49 Office: (303) 497-6615

50 Cell: (609) 375-6685

51 Fax: (303) 497-5318

52 E-mail: [cumulss@gmail.com](mailto:cumulss@gmail.com), [slee1247@umd.edu](mailto:slee1247@umd.edu)

**53 Abstract**

54

55 This study examines the ratio of ice crystal number concentration (ICNC) to cloud droplet  
56 number concentration (CDNC), which is ICNC/CDNC, in mixed-phase stratocumulus  
57 clouds. This examination is performed using a large-eddy simulation (LES) framework and  
58 one of efforts toward a more general understanding of mechanisms controlling cloud  
59 development, aerosol-cloud interactions and impacts of ice processes on them in mixed-  
60 phase stratocumulus clouds. For the examination, this study compares a case of polar  
61 mixed-phase stratocumulus clouds to that of midlatitude mixed-phase stratocumulus  
62 clouds with weak precipitation. It is found that ICNC/CDNC plays a critical role in making  
63 differences in cloud development with respect to the relative proportion of liquid and ice  
64 mass between the cases by affecting in-cloud latent-heat processes. Note that this  
65 proportion has an important implication for cloud radiative properties and thus climate. It  
66 is also found that ICNC/CDNC plays a critical role in making differences in interactions  
67 between clouds and aerosols and impacts of ice processes on clouds and their interactions  
68 with aerosols between the cases by affecting in-cloud latent-heat processes. Findings of  
69 this study suggest that ICNC/CDNC can be a simplified general factor that contributes to  
70 a more general understanding of mixed-phase clouds, their interactions with aerosols and  
71 roles of ice processes in them and thus, to the development of more general  
72 parameterizations of those clouds, interactions and roles.

73

74

75

76

77

78

79

80

81

82

83

## 1. Introduction

84

85

86 Stratiform clouds (e.g., stratus and stratocumulus clouds) have significant impacts on  
87 climate (Warren et al. 1986; Stephens and Greenwald 1991; Hartmann et al. 1992; Hahn  
88 and Warren 2007; Wood, 2012; Dione et al., 2019; Zheng et al., 2021). Since  
89 industrialization, aerosol concentrations have increased and this has had impacts on  
90 stratiform clouds and climate (Twomey, 1974; Albrecht, 1989; Ackerman et al., 2004).  
91 However, our level of understanding of these clouds and impacts has been low and this has  
92 caused the highest uncertainty in the prediction of future climate (Ramaswamy et al., 2001;  
93 Forster et al., 2007; Knippertz et al., 2011; Hannak et al., 2017). Stratiform clouds can be  
94 classified into warm and mixed-phase clouds. Mixed-phase clouds involve ice processes  
95 and frequently form in midlatitude and polar regions. Most previous studies have focused  
96 on warm clouds and their interactions with aerosols, whereas the mixed-phase clouds and  
97 their interactions with aerosols are poorly understood mainly due to the more complex ice  
98 processes. Hence, mixed-phase clouds and their interactions with aerosols account for the  
99 uncertainty more than warm clouds and their interactions with aerosols (Ramaswamy et al.,  
100 2001; Forster et al., 2007; Wood, 2012; IPCC, 2021; Li et al., 2022).

101 The relative proportion of liquid mass, which can be represented by liquid-water  
102 content (LWC) or liquid-water path (LWP), and ice mass, which can be represented by ice-  
103 water content (IWC) or ice-water path (IWP), in mixed-phase stratiform clouds plays a  
104 critical role in cloud radiative properties and thus their climate feedbacks (Choi et al., 2010  
105 and 2014; Zhang et al., 2019). This is because radiative properties of liquid particles are  
106 substantially different from those of ice particles. The relative proportion is defined to be  
107 IWC (IWP) over LWC (LWP) or  $IWC/LWC$  ( $IWP/LWP$ ) in this study. Motivated by this  
108 and the above-mentioned uncertainty, this study aims to improve our understanding of  
109 mixed-phase stratiform clouds and their interactions with aerosols with the emphasis on  
110 ice processes and  $IWC/LWC$  (or  $IWP/LWP$ ).

111 Lee et al. (2022) have investigated mixed-phase stratocumulus clouds in a midlatitude  
112 region and found that microphysical latent-heat processes are more important in the  
113 development of mixed-phase clouds and their interactions with aerosols than entrainment  
114 and sedimentation processes. Lee et al. (2022) have found that a microphysical factor, the

115 ratio of ice crystal number concentration (ICNC) to cloud droplet number concentration  
116 (CDNC) or ICNC/CDNC, play an important role in latent processes, the development of  
117 mixed-phase clouds and their interactions with aerosols. In particular, Lee et al. (2022)  
118 have found that IWC/LWC or IWP/LWP is strongly affected by ICNC/CDNC. This is  
119 because deposition (condensation) of water vapor occurs on the surface of ice crystals  
120 (droplets). Thus, ice crystals (droplets) act as sources of deposition (condensation) and then  
121 IWC or IWP (LWC or LWP). More ice crystals (droplets) provide the greater integrated  
122 surface area of ice crystals (droplets) and induce more deposition (condensation) for a  
123 given environmental condition (Lee et al., 2009; Khain et al., 2012; Fan et al., 2018; Chua  
124 and Ming, 2020; Lee et al., 2022). Note that deposition and condensation are processes  
125 through which water vapor is removed, hence ice crystals and droplets are sinks of water  
126 vapor when deposition and condensation occur. However, when it comes to deposition and  
127 condensation themselves as microphysical processes, ice crystals (droplets) can be  
128 considered the sources of deposition and condensation. The higher ICNC/CDNC means  
129 more ice crystals or sources of deposition per a droplet as a source of condensation in a  
130 given group of ice crystals and droplets. Thus, the higher ICNC/CDNC enables more  
131 deposition per unit condensation to occur, which can raise IWC/LWC or IWP/LWP.

132 Mixed-phase stratocumulus clouds in different regions are known to have different  
133 IWC/LWC or IWP/LWP and aerosol-cloud interactions (e.g., Choi et al., 2010 and 2014;  
134 Zhang et al., 2019). Lots of factors such as environmental conditions, which can be  
135 represented by variables such as temperature, humidity and wind shear, can explain those  
136 differences. Choi et al. (2010 and 2014) and Zhang et al. (2019) have shown that as  
137 temperature lowers, IWC/LWC or IWP/LWP tends to increase and indicated that  
138 temperature is a primary environmental condition to explain the differences in IWC/LWC  
139 among different regions or clouds. However, Choi et al. (2010 and 2014) and Zhang et al.  
140 (2019) have not discussed process-level mechanisms that govern the role of temperature in  
141 those differences.

142 It is important to establish a general principle that explains the differences in  
143 LWC/LWC and aerosol-cloud interactions among regions, since the general principle is  
144 useful in the development of a more general or comprehensive parameterization of  
145 stratocumulus clouds and their interactions with aerosols for climate models. This

146 contributes to the better prediction of future climate, considering that the absence of the  
147 comprehensive parameterization has been considered one of the biggest obstacles to the  
148 better prediction (Ramaswamy et al., 2001; Foster et al., 2007; Stevens and Feingold, 2009).

149 As a way of contributing to the establishment of the general principle, this study  
150 attempts to take ICNC/CDNC as a general factor, which can constitute the general principle,  
151 to explain the differences in IWC/LWC (or IWP/LWP) and aerosol-cloud interactions  
152 among clouds. This study also attempts to elucidate how ice processes differentiate mixed-  
153 phase clouds from warm clouds in terms of cloud development and its interactions with  
154 aerosols, and how this differentiation varies among cases of mixed-phase clouds with  
155 different ICNC/CDNC values. This attempt is valuable, considering that in general, the  
156 establishment of the general principle for stratocumulus clouds and their interactions with  
157 aerosols has been progressed much less than that for other types of clouds such as  
158 convective clouds and their interactions with aerosols. The attempt is valuable, also  
159 considering that our level of understanding of how ice processes differentiate mixed-phase  
160 clouds and their interactions with aerosols from much-studied warm clouds and their  
161 interactions with aerosols has been low. Here, we want to emphasize that this study does  
162 not aim to gain a fully established general principle, but aims to test the factor that can be  
163 useful to move ahead on our path to a more complete general principle. Hence, this study  
164 should be regarded a steppingstone to the established principle, and should not be  
165 considered a perfect study that get us the fully established principle. Taking into account  
166 the fact that even attempts to provide general factors for the general principle have been  
167 rare, the fulfilment of the aim is likely to provide us with valuable preliminary information  
168 that streamlines the development of a more established general principle.

169 For the attempt, this study investigates a case of mixed-phase stratiform clouds in the  
170 polar region. Via the investigation, this study aims to identify process-level mechanisms  
171 that control the development of those clouds and their interactions with aerosols, and the  
172 impact of ice processes on the development and interactions using a large-eddy simulation  
173 (LES) framework. Then, this study compares the mechanisms in the case of polar clouds  
174 to those in a case of midlatitude clouds which have been examined by Lee et al. (2022).  
175 This comparison is based on Choi et al. (2010 and 2014) and Zhang et al. (2019) which  
176 have shown that temperature is an important factor which explains the differences in

177 IWC/LWC among regions or clouds. Due to significant differences in latitudes, noticeable  
178 differences in the temperature of air are between the polar and midlatitude cases. Hence,  
179 through this comparison, this study looks at the role of temperature in those differences in  
180 IWC/LWC and associated aerosol-cloud interactions. More importantly than that, as a way  
181 of identifying process-level mechanisms that control the role of temperature, this study  
182 tests how ICNC/CDNC as the general factor is linked to the role of temperature, using the  
183 LES framework. Through this test, this study also identifies process-level mechanisms that  
184 control how ICNC/CDNC affects roles of ice processes in the differentiation between  
185 mixed-phase and warm clouds in terms of cloud development and its interactions with  
186 aerosols, and causes the variation of the differentiation between the cases of mixed-phase  
187 stratiform clouds.

188

## 189 **2. Case, model and simulations**

190

### 191 **2.1 LES model**

192

193 LES simulations are performed by using the Advanced Research Weather Research and  
194 Forecasting (ARW) model. A bin scheme, which is detailed in Khain et al. (2000) and  
195 Khain et al. (2011), is adopted by the ARW for the simulation of microphysics. Size  
196 distribution functions for each class of hydrometeors, which are classified into water drops,  
197 ice crystals (plate, columnar and branch types), snow aggregates, graupel and hail, and  
198 aerosols acting as cloud condensation nuclei (CCN) and ice-nucleating particles (INP) are  
199 represented with 33 mass doubling bins, i.e., the mass of a particle  $m_k$  in the  $k$ th bin is  
200 determined as  $m_k = 2m_{k-1}$ . Each of hydrometeors has its own terminal velocity that varies  
201 with the hydrometeor mass and the sedimentation of hydrometeors is simulated using their  
202 terminal velocity. The evolution of aerosol size distribution at each grid point is controlled  
203 by aerosol sinks and sources such as aerosol advection, turbulent mixing and activation. It  
204 is assumed that aerosols do not fall down by themselves and move around by airflow that  
205 is composed of horizontal flow, updrafts, downdrafts and turbulent motions. When aerosols  
206 move with airflow, it is assumed that they move with the same velocity as airflow. Taking  
207 activation as an example of the evolution of aerosol size distribution, the bins of the aerosol

208 spectra that correspond to activated particles are emptied. Activated aerosol particles are  
209 included in hydrometeors and move to different classes and sizes of hydrometeors through  
210 collision-coalescence. In case hydrometeors with aerosol particles precipitate to the surface,  
211 those particles are removed from the atmosphere.

212 The large energetic turbulent eddies are directly resolved by the LES framework, and  
213 the effects of the smaller subgrid-scale turbulent motions on the resolved flow are  
214 parameterized based on the most widely used method that Smagorinsky (1963) and Lilly  
215 (1967) proposed. In this method, the mixing time scale is defined to be the norm of the  
216 strain rate tensor (Bartosiewicz and Duponcheel, 2018). A cloud-droplet nucleation  
217 parameterization based on Köhler theory represents cloud-droplet nucleation. Arbitrary  
218 aerosol mixing states and aerosol size distributions can be fed to this parameterization. To  
219 represent heterogeneous ice-crystal nucleation, the parameterizations by Lohmann and  
220 Diehl (2006) and Möhler et al. (2006) are used. In these parameterizations, contact,  
221 immersion, condensation-freezing, and deposition nucleation paths are all considered by  
222 taking into account the size distribution of INP, temperature and supersaturation.  
223 Homogeneous aerosol (or haze particle) and droplet freezing is  
224 also considered following the theory developed by Koop et al. (2000).

225 The bin microphysics scheme is coupled to the Rapid Radiation Transfer Model  
226 (RRTM; Mlawer et al., 1997). The effective sizes of hydrometeors, which are calculated  
227 in the bin scheme, are fed into the RRTM as a way of considering effects of the effective  
228 sizes on radiation. The surface process and resultant surface heat fluxes are simulated by  
229 the interactive Noah land surface model (Chen and Dudhia, 2001).

230

## 231 **2.2 Case and simulations**

232

### 233 **2.2.1 Case and standard simulations**

234

235 In the Svalbard area, Norway, a system of mixed-phase stratocumulus clouds existed over  
236 the horizontal domain marked by a red rectangle in Figure 1 and a period between ~02:00  
237 local solar time (LST) and 10:00 LST on March 29<sup>th</sup>, 2017. These clouds are observed by  
238 ground radar and lidar and these radar and lidar are a part of the Cloudnet ground



239 observation that is deployed at a location in the red rectangle. The Cloudnet ground  
240 observation is composed of a suite of instruments such as lidar, radar and radiometer and  
241 described in Hogan et al. (2006). On average, the bottom and top of these clouds are at  
242  $\sim 400$  m and  $\sim 3$  km in altitude, respectively, according to observation by those radar and  
243 lidar. The simulation of the observed system or case, i.e., the control run, is performed  
244 three-dimensionally over the red rectangle and the period. The horizontal domain adopts  
245 a 100-m resolution for the control run. The length of the domain in the horizontal directions  
246 is 50 km. The length of the domain in the vertical direction is  $\sim 5$  km and the resolution for  
247 the vertical domain gets coarsened with height from  $\sim 20$  m just above the surface to  $\sim 100$   
248 m at the model top. Reanalysis data, which are produced by Met Office Unified Model  
249 (Brown et al., 2012) every 6 hours on a  $0.11^\circ \times 0.11^\circ$  grid, provide potential temperature,  
250 specific humidity, and wind as initial and boundary conditions, which represent synoptic-  
251 scale environment, for the control run. The control run employs an open lateral boundary  
252 condition. Figure 2a shows the vertical distribution of the domain-averaged potential  
253 temperature and humidity in those reanalysis data at the first time step. A neutral, mixed  
254 layer is between the surface and 1 km in altitude as an initial condition (Figure 2a). Figure  
255 2b shows the time evolution of the domain-averaged large-scale subsidence or downdraft  
256 in the reanalysis data and at the model top. The large-scale subsidence gradually reduces  
257 with time (Figure 2b). Figure 2c shows the time evolution of the domain-averaged surface  
258 temperature in the reanalysis data. This evolution of the surface temperature is mostly  
259 controlled by the sea surface temperature (SST) considering that most portion of the red-  
260 rectangle domain is accounted for by the ocean (Figure 1). Between  $\sim 06:00$  LST around  
261 when the sun rises and  $\sim 08:00$  LST, the surface temperature increases from  $-2.2$  to  $-1.6$   $^\circ\text{C}$ ,  
262 and after that, it does not show significant increase or decrease (Figure 2c).

263 The properties of cloud condensation nuclei (CCN) such as the number concentration,  
264 size distribution and composition are measured in the domain (Tunved et al., 2013; Jung et  
265 al., 2018). The measurement indicates that on average, aerosol particles are an internal  
266 mixture of 70 % ammonium sulfate and 30 % organic compound. This mixture is assumed  
267 to represent aerosol chemical composition over the whole domain and simulation period  
268 for this study. The observed and averaged concentration of aerosols acting as CCN is  $\sim 200$   
269  $\text{cm}^{-3}$  over the simulation period. Based on this,  $200 \text{ cm}^{-3}$  as an averaged concentration of

270 aerosols acting as CCN is interpolated into all of grid points immediately above the surface  
271 at the first time step.

272 This study does not take into account aerosol effects on radiation before aerosol is  
273 activated, since no significant amount of radiation absorbers is found in the mixture. Based  
274 on observation, the size distribution of aerosols acting as CCN is assumed to be a tri-modal  
275 log-normal distribution (Figure 3). The shape of distribution, which is a tri-modal log-  
276 normal distribution, as shown in Figure 3 is applied to the size distribution of aerosols  
277 acting as CCN in all parts of the domain during the whole simulation period. The assumed  
278 shape in Figure 3 is obtained by performing the average on the size distribution parameters  
279 (i.e., modal radius and standard deviation of each of nuclei, accumulation and coarse modes,  
280 and the partition of aerosol number among those modes) over the simulation period. This  
281 study takes an assumption that the interpolated CCN concentrations do not vary with height  
282 in a layer between the surface and the planetary boundary layer (PBL) top around 1 km in  
283 altitude. However, above the PBL top, they are assumed to decrease exponentially with  
284 height, although the shape of size distribution and composition do not change with height.  
285 It is assumed that the properties of INP and CCN are not different except for concentrations.  
286 The concentration of aerosols acting as CCN is assumed to be 100 times higher than that  
287 acting as INP over grid points at the first time step based on a general difference in  
288 concentrations between CCN and INP (Pruppacher and Klett, 1978). Hence, the  
289 concentration of aerosols acting as INP at the first time step is  $2 \text{ cm}^{-3}$  in the control run.  
290 This assumed concentration of aerosols acting as INP is higher than usual (Seinfeld and  
291 Pandis, 1998). However, Hartmann et al. (2021) observed the INP concentration that was  
292 higher than assumed here in the Svalbard area when strong dust events occur, meaning that  
293 the assumed INP concentration is not that unrealistic.

294 To examine effects of aerosols on mixed-phase clouds, the control run is repeated by  
295 increasing the concentration of aerosols by a factor of 10. In the repeated (control) run, the  
296 initial concentrations of aerosols acting as CCN and INP at grid points immediately above  
297 the surface are 2000 (200) and  $20 (2) \text{ cm}^{-3}$ , respectively. Reflecting these concentrations in  
298 the simulation name, the control run is referred to as “the 200\_2 run” and the repeated run  
299 is referred to as “the 2000\_20 run”. To isolate effects of aerosols acting as CCN (INP) on  
300 mixed-phase clouds, the control run is repeated again by increasing the concentration of

301 aerosols acting as CCN (INP) only but not INP (CCN) by a factor of 10. In this repeated  
302 run with the increase in the concentration of aerosols acting as CCN (INP), the initial  
303 concentrations of aerosols acting as CCN and IFN at grid points immediately above the  
304 surface are 2000 (200) and 2 (20)  $\text{cm}^{-3}$ , respectively. Reflecting this, the repeated run is  
305 referred to as “the 2000\_2 (200\_20) run”.

306

### 307 **2.2.2 Additional simulations**

308

309 To isolate impacts of ice processes on the adopted case and its interactions with aerosols,  
310 the 200\_2 and 2000\_2 runs are repeated by removing ice processes. These repeated runs  
311 are referred to as the 200\_2\_noice and 2000\_2\_noice runs. In the 200\_2\_noice and  
312 2000\_2\_noice runs, all hydrometeors (i.e., ice crystals, snow, graupel, and hail), phase  
313 transitions (e.g., deposition and sublimation) and aerosols (i.e., INP) which are associated  
314 with ice processes are removed. Hence, in these runs, only droplets (i.e., cloud liquid),  
315 raindrops, associated phase transitions (e.g., condensation and evaporation) and aerosols  
316 acting as CCN are present, regardless of temperature. Stated differently, these noice runs  
317 simulate the warm-cloud counterpart of the selected mixed-phase cloud system. Via  
318 comparisons between a pair of the 200\_2 and 2000\_2 runs and a pair of the 200\_2\_noice  
319 and 2000\_2\_noice runs, the role of ice processes in the differentiation between mixed-  
320 phase and warm clouds is to be identified. Along with this identification, the role of the  
321 interplay between ice crystals and droplets in the development of the selected mixed-phase  
322 cloud system and its interactions with aerosols is to be isolated.

323 As detailed in Sections 3.1.2 and 3.2.2 below, the test of ICNC/CDNC as a general  
324 factor requires more simulations to see impacts of ICNCavg/CDCNavg on clouds and their  
325 interactions with aerosols. Here, ICNCavg (CDNCavg) represents the average ICNC  
326 (CDNC) over grid points and time steps with non-zero ICNC (CDNC).  
327 ICNCavg/CDNCavg represents overall ICNC/CDNC over the domain and simulation  
328 period. To respond to this requirement, 200\_2\_fac10, 200\_2\_fac10\_CCN10,  
329 200\_2\_fac10\_INP10 runs are performed and their details are given in Sections 3.1.2 and  
330 3.2.2. In addition, all the simulations above are repeated by turning off radiative processes  
331 and Section 3.3 provides the details of these repeated simulations. These repeated runs are

332 the 200\_2\_norad, 2000\_20\_norad, 2000\_2\_norad, 200\_20\_norad, 200\_2\_noice\_norad,  
333 2000\_2\_noice\_norad, 200\_2\_fac10\_norad, 200\_2\_fac10\_CCN10\_norad and  
334 200\_2\_fac10\_INP10\_norad runs. Moreover, based on the argument in Section 4.2, the  
335 4000\_45, 13\_0.1, 4000\_1.8\_fac10 and 12\_0.0035\_fac10 runs are performed and details of  
336 these runs are provided in Section 4.2. The summary of simulations in this study is given  
337 in Table 1.

338

### 339 3. Results

340

#### 341 3.1 The 200\_2 run vs. the 200\_2\_noice run

342

343 This study adopts the Cloudnet ground observation to evaluate the 200\_2 run. Observed  
344 LWP is provided by radiometer. The retrieval of IWP is performed by using radar  
345 reflectivity and lidar backscatter as described in Donovan et al. (2001), Donovan (2003)  
346 and Tinel et al. (2005). As mentioned above, observed cloud-bottom and -top heights are  
347 obtained from radar and lidar measurements. Simulated LWP and IWP, as shown in Figure  
348 4 and Table 2, are compared to the observed LWP and retrieved IWP, respectively. The  
349 average LWP over all time steps and grid columns is 1.23 in the 200\_2 run and 1.12 in  
350 observation. The average IWP over all time steps and grid columns is 31.94 in the 200\_2  
351 run and 29.10 in retrieval. Cloud-bottom height, which is averaged over grid columns and  
352 time steps with non-zero cloud-bottom height, is 420 and 440 m in the 200\_2 run and  
353 observation, respectively. Cloud-top height, which is averaged over grid columns and time  
354 steps with non-zero cloud-top height, is 3.5 and 3.3 km in the 200\_2 run and observation,  
355 respectively. Each of LWP, cloud-bottom and -top heights shows an ~10% difference  
356 between the 200\_2 run and observation. IWP also shows an ~10% difference between the  
357 200\_2 run and retrieval. Thus, the 200\_2 run is considered performed reasonably well for  
358 these variables.

359 To provide additional or supplementary information of cloud development, the time  
360 evolution of the simulated and observed cloud-top height is shown together with the  
361 simulated evolution of the surface sensible and latent-heat fluxes in Supplementary Figure  
362 1. This is based on the fact that the cloud-top height is considered a good indicative of

363 cloud development and the surface fluxes are considered important parameters controlling  
364 the overall development of clouds. Simulated evolutions in Supplementary Figure 1 are  
365 from the 200\_2 run. The cloud-top height increases between 02:00 and ~05:00 LST and  
366 after ~05:00 LST, it reduces gradually. The surface fluxes reduce with time, although the  
367 reduction rate of the fluxes starts to decrease around 08:00 LST in association with the  
368 increase in the surface temperature between ~06:00 and ~08:00 LST as shown in Figure  
369 2c.

370 The time- and domain-averaged IWP (IWC) is ~one order of magnitude greater than  
371 LWP (LWC) in the 200\_2 run (Figure 4 and Table 2). For the sake of simplicity, the  
372 averaged IWC (IWP) over the averaged LWC (LWP) is denoted by IWC (IWP)/LWC  
373 (LWP), henceforth. IWC/LWC and IWP/LWP are 26.28 and 25.96, respectively, in the  
374 200\_2 run. Since IWP and LWP are vertically integrated IWC and LWC over the vertical  
375 domain, respectively, the qualitative nature of differences between IWC and LWC is not  
376 much different from that between IWP and LWP. Hence, mentioning both a pair of IWC  
377 and LWC and that of IWP and LWP is considered redundant, and mentioning either a pair  
378 of IWC and LWC or that of IWP and LWP enhances the readability. Henceforth, IWC and  
379 LWC are chosen to be mentioned in text, although all of IWC, LWC, IWP and LWP are  
380 displayed in Tables 2 and 3.

381 Choi et al. (2014) and Zhang et al. (2019) have obtained the supercooled cloud fraction  
382 (SCF), which is basically the ratio of LWC to the sum of LWC and IWC and denoted by  
383  $LWC/(LWC+IWC)$ , using satellite- and ground-observed data collected over the period of  
384 ~5 years and ~1 year, respectively. Choi et al. (2014) have shown that SCF is as low as  
385 ~0.01 for the temperature range between -16 and -33 °C. Zhang et al. (2019) have also  
386 shown that SCF is as low as ~0.03 for the same temperature range, although the occurrence  
387 of SCF of ~0.03 or lower is rare. Note that the average air temperature immediately below  
388 the cloud base and above the cloud top over the simulation period is -16 and -33 °C,  
389 respectively, in the 200\_2 run, and SCF in the 200\_2 run is 0.04. Hence, based on Choi et  
390 al. (2014) and Zhang et al. (2019), we believe that SCF in the 200\_2 run is observable and  
391 thus not that unrealistic, although it may not occur frequently.

392 To understand process-level mechanisms that control the results, microphysical  
393 processes are analyzed. As indicated by Ovchinnikov et al. (2011), in clouds with weak

394 precipitation, a high-degree correlation is found between IWC and deposition or between  
395 LWC and condensation, considering that deposition and condensation are sources of IWC  
396 and LWC, respectively. In the 200\_2 run, the average surface precipitation rate over the  
397 simulation period is  $\sim 0.0020 \text{ mm hr}^{-1}$ , which can be considered weak. Hence, in this case,  
398 condensation and deposition are considered proxies for IWC and LWC, respectively. Based  
399 on this, to gain a process-level understanding of microphysical processes that control the  
400 simulated IWC and LWC, condensation and deposition are analyzed.

401 As seen in Figure 5 and Table 2, the average deposition rate is  $\sim$ one order of magnitude  
402 greater than condensation rate in the 200\_2 run, leading to much greater IWC than LWC  
403 in the 200\_2 run. This is in contrast to the situation in the case of mixed-phase  
404 stratocumulus clouds, which were located in a midlatitude region, in Lee et al. (2022). In  
405 this case, the average IWC and LWC are at the same order of magnitude. For the sake of  
406 brevity, this case in Lee et al. (2022) is referred to as “the midlatitude case”, while the case  
407 of mixed-phase clouds, which is adopted by this study, in the Svalbard area is referred to  
408 “the polar case”, henceforth. In the midlatitude case, IWC/LWC is 1.55, which is  $\sim$  one  
409 order of magnitude smaller than that in the polar case.

410 Warm clouds in the 200\_2\_noice run shows that the time- and domain-averaged  
411 condensation rate that is lower than the time- and the domain-averaged sum of  
412 condensation and deposition rates in the 200\_2 run (Figure 5 and Table 2). This leads to a  
413 situation where warm clouds in the 200\_2\_noice run shows the time- and domain-averaged  
414 LWC that is lower than the time- and domain-averaged water content (WC), which is the  
415 sum of IWC and LWC, in mixed-phase clouds in the 200\_2 run (Figure 4 and Table 2).  
416 This is despite the fact that LWC in the 200\_2\_noice run is higher than LWC in the 200\_2  
417 run (Figure 4 and Table 2); WC represents the total cloud mass in mixed-phase clouds,  
418 while LWC alone represents the total cloud mass in warm clouds.

419 It should be noted that the average rate of sedimentation of droplets over the cloud  
420 base and simulation period reduces from the 200\_2\_noice run to the 200\_2 run (Table 2).  
421 This is mainly due to the decrease in LWC from the 200\_2\_noice run to the 200\_2 run.  
422 The average rate of sedimentation of ice crystals over the cloud base and simulation period  
423 increases from the 200\_2\_noice run to the 200\_2 run, since sedimentation of ice crystals is  
424 absent in the 200\_2\_noice run (Table 2). The average entrainment rate over the cloud top

425 and simulation period increases from the 200\_2\_noice run to the 200\_2 run (Table 2).  
426 Hence, the droplet sedimentation tends to increase the total cloud mass in the 200\_2 run,  
427 and the ice-crystal sedimentation and entrainment tend to reduce the total cloud mass in  
428 the 200\_2 run, as compared to that in the 200\_2\_noice run. This means that the droplet  
429 sedimentation contributes to increase in the total cloud mass from the 200\_2\_noice run to  
430 the 200\_2 run, while entrainment and the ice-crystal sedimentation counter the increase.  
431 Thus, entrainment and the ice-crystal sedimentation should be opted out when it comes to  
432 mechanisms leading to the increase in the total cloud mass. Here, the vertical integration  
433 of each of condensation and deposition rates is obtained over each cloudy column in the  
434 domain for each of the runs. For the sake of the brevity, this vertical integration of  
435 condensation (deposition) rate is referred to as the integrated condensation (deposition)  
436 rate. Then, each of the integrated condensation and deposition rates is averaged over cloudy  
437 columns and the simulation period. It is found that the change in the average rate of the  
438 droplet sedimentation over the cloud base and simulation period from the 200\_2\_noice run  
439 to the 200\_2 run is ~five to six orders of magnitude smaller than that in the average  
440 integrated condensation rate, the average integrated deposition rate, and the sum of the  
441 average integrated condensation and deposition rate (Table 2). Thus, condensation and  
442 deposition, but not the droplet sedimentation, are main factors controlling differences in  
443 cloud mass, which is represented by LWC and IWC, and in the total cloud mass between  
444 the 200\_2 and 200\_2\_noice runs as are between the midlatitude case and its warm-cloud  
445 counterpart.

446

447

### 3.1.1 Hypothesis

448

449 We hypothesized that ICNC/CDNC can be an important factor that determines above-  
450 described differences between the polar and midlatitude cases. Remember that ice crystals  
451 are more as sources of deposition per a droplet when ICNC/CDNC is higher. Thus, when  
452 ICNC/CDNC is higher and  $q_v > q_{sw}$ , it is more likely that more portion of water vapor is  
453 deposited onto ice crystals by stealing water vapor, which is supposed to be condensed  
454 onto droplets, from droplets in an air parcel. Here,  $q_v$  and  $q_{sw}$  represent water-vapor  
455 pressure and water-vapor saturation pressure for liquid water or droplets, respectively.

456 When ICNC/CDNC is higher and  $q_{si} < q_v < q_{sw}$ , more ice crystals can absorb water vapor,  
457 including that which is produced by droplet evaporation, per a droplet; here,  $q_{si}$  represents  
458 water-vapor saturation pressure for ice water or ice crystals. Thus, with higher  
459 ICNC/CDNC, it is more likely that that more portion of water vapor is deposited onto ice  
460 crystals in an air parcel as shown in Lee et al. (2022).

461 ICNC<sub>avg</sub>/CDNC<sub>avg</sub> is 0.22 in the control run (i.e., the 200\_2 run) for the polar case  
462 and 0.019 in the control run for the midlatitude case which is described in Lee et al. (2022).  
463 Henceforth, the control run for the midlatitude case is referred to as the control-midlatitude  
464 run. ICNC<sub>avg</sub>/CDNC<sub>avg</sub> is ~one order of magnitude higher for the polar case than for the  
465 midlatitude case. This is despite the fact that the ratio of the initial number concentration  
466 of aerosols acting as INP to that of acting as CCN is identical between the 200\_2 and  
467 control-midlatitude runs. This is mainly due to the fact that ice nucleation strongly depends  
468 on air temperature (Prappacher and Klett, 1978). When supercooling is stronger, in general,  
469 more ice crystals are nucleated for a given group of aerosols acting as INP. The average  
470 air temperature immediately below the cloud base over the simulation period is -16 °C in  
471 the 200\_2 run and -5 °C in the control-midlatitude run. The average air temperature  
472 immediately above the cloud top is -33 °C in the 200\_2 run and -15 °C in the control-  
473 midlatitude run. Hence, supercooling is greater and this contributes to the higher  
474 ICNC<sub>avg</sub>/CDNC<sub>avg</sub> in the polar case than in the midlatitude case. The higher  
475 ICNC<sub>avg</sub>/CDNC<sub>avg</sub> is likely to induce more portion of water vapor to be deposited onto  
476 ice crystals in the polar case than in the midlatitude case. It is hypothesized that this in turn  
477 enables IWC/LWC in the 200\_2 run to be one order of magnitude greater than that in the  
478 control-midlatitude run or in the midlatitude case. Much higher IWC than LWC, which  
479 results in a much higher IWC/LWC in the polar case than in the midlatitude case, in the  
480 200\_2 run overcomes lower LWC in the 200\_2 run than that in the 200\_2\_noice run, which  
481 leads to the greater total cloud mass in the 200\_2 run than in the 200\_2\_noice run (Figure  
482 4 and Table 2). However, IWC whose magnitude is similar to the magnitude of LWC,  
483 which results in a much lower IWC/LWC in the midlatitude case than in the polar case, in  
484 the midlatitude case is not able to overcome lower LWC in the midlatitude case than that  
485 in the midlatitude warm clouds, which leads to the greater total cloud mass in the  
486 midlatitude warm clouds than in the midlatitude case; here, the midlatitude warm clouds



487 are generated by removing ice processes in the midlatitude case. This means that associated  
488 with higher ICNC/CDNC and IWC/LWC, ice processes enhance the total cloud mass for  
489 the polar case as compared to that for the polar warm-cloud counterpart. However, in the  
490 midlatitude case, associated with lower ICNC/CDNC and IWC/LWC, ice processes reduce  
491 the total cloud mass as compared to that for the midlatitude warm-cloud counterpart.

492

### 493 **3.1.2 Role of ICNC/CDNC**

494

495 To test the hypothesis above about the role of ICNC/CDNC in above-described differences  
496 between the polar and midlatitude cases, the 200\_2 run is repeated by reducing  
497 ICNCavg/CDNCavg by a factor of 10. This is done by reducing the concentration of  
498 aerosols acting as INP but not CCN in a way that ICNCavg/CDNCavg is lower by a factor  
499 of 10 in the repeated run than in the 200\_2 run. In this way, this repeated run has  
500 ICNCavg/CDNCavg at the same order of magnitude as that in the control-midlatitude run.  
501 This repeated run is referred to as the 200\_2\_fac10 run. As shown in Figure 6 and Table 2,  
502 the 200\_2\_fac10 run shows much lower deposition rate and IWC than the 200\_2 run does.  
503 However, as we move from the 200\_2 run to the 200\_2\_fac10 run, the time- and domain-  
504 averaged condensation rate and LWC increases (Figure 6 and Table 2). This is because  
505 reduction in deposition increases the amount of water vapor, which is not consumed by  
506 deposition but available for condensation. Associated with this, in the 200\_2\_fac10 run,  
507 the time- and domain-averaged deposition rate and IWC become similar to the average  
508 condensation rate and LWC, respectively (Figure 6 and Table 2). Hence, IWC/LWC  
509 reduces from 26.28 in the 200\_2 run to 1.05 in the 200\_2\_fac10 run as ICNCavg/CDNCavg  
510 reduces from the 200\_2 run to the 200\_2\_fac10 run. Here, IWC/LWC in the 200\_2\_fac10  
511 run is similar to that in the midlatitude-control run, which demonstrate that the difference  
512 in ICNC/CDNC is able to explain the difference in IWC/LWC between the polar and  
513 midlatitude cases. It is notable that the reduction in deposition is dominant over the increase  
514 in condensation with the decrease in ICNCavg/CDNCavg. Hence, the sum of condensation  
515 and deposition rates and WC reduce from the 200\_2 run to the 200\_2\_fac10 run. That the  
516 sum of condensation and deposition rates and WC reduce in a way that the sum and WC in  
517 the mixed-phase clouds in the 200\_2\_fac10 run are lower than condensation rate and LWC,

518 respectively, in the warm clouds in the 200\_2\_noice run is also notable (Figure 6 and Table  
519 2). This is similar to the situation in the midlatitude case and thus demonstrates that the  
520 different relation between the mixed-phase and warm clouds can be associated with the  
521 difference in ICNC/CDNC between the polar and midlatitude cases.

522 The rate of the sedimentation of ice crystals at the cloud base reduces as  
523 ICNCavg/CDNCavg reduces between the 200\_2 and 200\_2\_fac10 runs, mainly due to  
524 reduction in the ice-crystal mass (Table 2). The rate of droplet sedimentation at the cloud  
525 base increases as ICNCavg/CDNCavg reduces mainly due to increases in droplet mass and  
526 size in association with the increases in LWC (Table 2). The entrainment rate at the cloud  
527 top reduces as ICNCavg/CDNCavg reduces (Table 2). Hence, the changing sedimentation  
528 tends to reduce LWC and increase IWC, while the changing entrainment tends to increase  
529 the total cloud mass or WC with the reducing ICNCavg/CDNCavg. Hence, changes in the  
530 sedimentation counter the increase in LWC, and the decrease in IWC with the reducing  
531 ICNCavg/CDNCavg. Changes in the entrainment counters the decrease in WC with the  
532 reducing ICNCavg/CDNCavg between the 200\_2 and 200\_2\_fac10 runs. Here, we see that  
533 changes in the sedimentation and entrainment are not factors that lead to the increase in  
534 LWC, and the decrease in IWC, and eventually the decrease in WC with the reducing  
535 ICNCavg/CDNCavg. The analysis of the sedimentation and entrainment exclude them  
536 from factors inducing above-described differences between the 200\_2 and 200\_2\_fac10  
537 runs. Instead, this analysis grants more confidence in the fact that deposition and  
538 condensation, which are strongly dependent on ICNC/CDNC, are main factors inducing  
539 those differences.

540

### 541 **3.2 Aerosol-cloud interactions**

542

543 Comparisons between the 200\_2 and 2000\_20 runs show that with the increasing  
544 concentration of both of aerosols acting as CCN and those as INP, IWC increases but LWC  
545 decreases in the polar case (Figures 7 and Table 2). These decreases in LWC are negligible  
546 as compared to these increases in IWC. Hence, the increases in IWC outweigh the  
547 decreases in LWC, leading to aerosol-induced increases in WC (Figures 7 and Table 2).  
548 To identify roles of specific types of aerosols in these aerosol-induced changes,

549 comparisons not only between the 200\_2 and 200\_20 runs but also between the 200\_2 and  
550 2000\_2 runs are performed. Comparisons between the 200\_2 and 200\_20 runs show that  
551 the increasing concentration of aerosols acting as INP induces increases in IWC but  
552 decreases in LWC (Figure 7 and Table 2). The magnitudes of these increases and decreases  
553 are similar to those between the 200\_2 and 2000\_20 runs (Figure 7 and Table 2). However,  
554 comparisons between the 200\_2 and 2000\_2 runs show that the increasing concentration  
555 of aerosols acting as CCN induces negligible changes in either IWC or LWC. Thus, CCN-  
556 induced changes in the total cloud mass are negligible, although the increasing  
557 concentration of aerosols acting as CCN induces a slight decrease in IWC, and a slight  
558 increase in LWC (Figure 7 and Table 2). This demonstrates that INP plays a much more  
559 important role than CCN when it comes to the response of the total cloud mass to increasing  
560 aerosol concentrations. However, in the midlatitude case, the increasing concentration of  
561 aerosols acting as CCN generates changes in the mass as significantly as the increasing  
562 concentration of aerosols acting as INP does.

563 To identify roles played by ice processes in aerosol-cloud interactions, a pair of the  
564 200\_2\_noise and 2000\_2\_noise runs are analyzed and compared to the previous four  
565 standard simulations (i.e., the 200\_2, 200\_20, 2000\_2 and 2000\_20 runs). The CCN-  
566 induced increases in LWC in those noise runs are much greater than the CCN-induced  
567 changes in WC in the 200\_2 and 2000\_2 runs (Figure 7 and Table 2). However, these CCN-  
568 induced increases in LWC in the noise runs are smaller than the INP-induced increases in  
569 WC in the 200\_2 and 200\_20 runs (Figure 7 and Table 2). This is different from the  
570 midlatitude case where changes in the total cloud mass, whether they are induced by the  
571 increasing concentration of aerosols acting as CCN or INP, in the mixed-phase clouds are  
572 much lower than those CCN-induced changes in the warm clouds.

573

### 574 **3.2.1 Deposition, condensation, sedimentation and entrainment**

575

576 The CCN-induced increases (decreases) in condensation (deposition) rate are negligible,  
577 leading to the CCN-induced negligible increases (decreases) in LWC (IWC) between the  
578 200\_2 and 2000\_2 runs (Figure 7 and Table 2). However, between the 200\_2 and 200\_20  
579 runs, rather the significant INP-induced increases are in deposition rate, leading to the

580 significant INP-induced increases in IWC (Figure 7 and Table 2). Between the 200\_2 and  
581 200\_20 runs, INP-induced decreases in condensation rate are negligible, leading to the  
582 negligible INP-induced decreases in LWC, as compared to the INP-induced increases in  
583 deposition rate and IWC (Figure 7 and Table 2). With the increasing concentration of  
584 aerosols acting as INP from the 200\_2 run to the 200\_20 run, the sedimentation of ice  
585 crystals at the cloud base decreases (Table 2). This is mainly due to decreases in the size  
586 of ice crystals in association with increases INP and resultant increases in ICNC. From the  
587 200\_2 run to the 200\_20 run, the sedimentation of droplets at the cloud base decreases as  
588 shown in Table 2, mainly due to decreases in LWC. From the 200\_2 run to the 200\_20 run,  
589 the entrainment at the cloud top increases (Table 2). Hence, the INP-induced changes in  
590 the sedimentation contribute to the INP-induced increases in IWC but counter the INP-  
591 induced reduction in LWC. The entrainment counters the INP-induced increases in WC.  
592 Hence, we see that changes in entrainment and the droplet sedimentation are not factors  
593 that lead to the INP-induced increases in WC and decreases in LWC, respectively. The  
594 INP-induced increases in deposition and decreases in the sedimentation of ice crystals both  
595 contribute to the INP-induced increases in IWC. However, the INP-induced changes in the  
596 average integrated deposition rate over cloudy columns and the simulation period is ~ four  
597 orders of magnitude greater than those in the average rate of ice-crystal sedimentation over  
598 the cloud base and simulation period (Table 2). Hence, the role of the ice-crystal  
599 sedimentation in the INP-induced changes in IWC is negligible as compared to that of  
600 deposition.

601 In the warm clouds in the 200\_2\_noice and 2000\_2\_noice runs, the CCN-induced  
602 increases in condensation rate occur, leading to those in LWC (Figure 7 and Table 2).  
603 However, the CCN-induced increases in condensation rate in the warm clouds associated  
604 with the polar case are lower than the INP-induced increases in deposition rate in the polar  
605 case (Table 2). This contributes to aerosol-induced smaller changes in the total cloud mass  
606 in the polar warm clouds than in the polar mixed-phase clouds. The sedimentation of  
607 droplets at the cloud base reduces and the entrainment at the cloud top increases from the  
608 200\_2\_noice run to 2000\_2\_noice run (Table 2). The increasing concentration of aerosols  
609 acting as CCN induces increases in CDNC and decreases in the droplet size, leading to the  
610 reduction in the droplet sedimentation from the 200\_2\_noice run to 2000\_2\_noice run. The

611 CCN-induced changes in the sedimentation contribute to the CCN-induced increases in  
612 LWC. The entrainment counters the CCN-induced increases in LWC. Hence, the  
613 entrainment is not a factor which induces the CCN-induced increases in LWC between the  
614 200\_2\_noice and 2000\_2\_noice runs. As seen in Table 2, the CCN-induced changes in the  
615 sedimentation rate are ~three orders of magnitude smaller than those in the integrated  
616 condensation rate. Hence, the role of sedimentation in changes in LWC or WC between  
617 the 200\_2\_noice and 2000\_2\_noice runs is negligible as compared to that of condensation.

618

### 619 **3.2.2 Understanding differences between the polar and midlatitude cases**

620

621 Roughly speaking, the CCN-(INP-)induced changes in LWC (IWC) via CCN-  
622 (INP-)induced changes in autoconversion of droplets (ice crystals) are proportional to  
623 LWC (IWC) that changing CCN (INPs) affect (e.g., Liu and Daum, 2004; Kogan, 2013;  
624 Lee and Baik, 2017; Dudhia, 1989; Lim and Hong, 2010; Mansell et al. 2010). This is for  
625 given environmental conditions (e.g., temperature and humidity) and given CCN-  
626 (INP-)induced changes in microphysical factors such as sizes and number concentrations  
627 of droplets (ice crystals). Hence, in the polar case, with a given much lower LWC than  
628 IWC, the changing concentration of aerosols acting as CCN is likely to induce smaller  
629 changes in the given LWC via CCN impacts on the droplet autoconversion. This is as  
630 compared to changes in the given IWC which are induced by the changing concentration  
631 of aerosols acting as INP and thus changing ice-crystal autoconversion.

632 The smaller (larger) changes in the given LWC (IWC) are related to changes in CDNC  
633 (ICNC). These changes in CDNC (ICNC) are initiated by those in droplet (ice crystal)  
634 autoconversion. Changes in integrated droplet (ice-crystal) surface area, which are induced  
635 by those in CDNC (ICNC), initiate those in the given LWC (IWC). Remember that  
636 condensation (deposition) occurs on droplet (ice-crystal) surface and thus droplets (ice  
637 crystals) act as a source of condensation (deposition). Hence, those changes in CDNC  
638 (ICNC) and associated integrated droplet (ice-crystal) surface area can lead to changes in  
639 condensation (deposition) and thus feedbacks between condensation (deposition) and  
640 updrafts. The smaller CCN-induced changes in LWC involve changes in CDNC and  
641 associated smaller changes in condensation and feedbacks between condensation and

642 updrafts in the polar case. This is as compared to changes in deposition and feedbacks  
643 between deposition and updrafts which are associated with the INP-induced changes in  
644 ICNC and the related larger INP-induced changes in IWC in the polar case. The smaller  
645 CCN-induced changes in LWC involve smaller changes in water vapor that is consumed  
646 by droplets in the polar case. The larger INP-induced changes in IWC involve larger  
647 changes in water vapor that is consumed by ice crystals in the polar case. This leaves the  
648 CCN-induced smaller changes in the amount of water vapor available for deposition, which  
649 induce the smaller CCN-induced changes in IWC in the polar case. This is as compared to  
650 the INP-induced changes in the amount of water vapor which is available for condensation  
651 and associated changes in LWC in the polar case.

652       The lower LWC in the polar warm clouds than IWC in the polar case contributes to the  
653 INP-induced greater changes in IWC than the CCN-induced changes in LWC in the polar  
654 warm clouds. The lower LWC in the polar case than that in the polar warm clouds  
655 contributes to the CCN-induced greater changes in LWC in the polar warm clouds than  
656 those in LWC and subsequent changes in IWC in the polar case.

657       In contrast to the situation in the polar case, in the midlatitude case, remember that a  
658 given LWC is at the same order of magnitude of IWC. Hence, the CCN- induced changes  
659 in LWC and subsequent changes in IWC are similar to the INP-induced changes in IWC  
660 and subsequent changes in LWC. The greater LWC in the midlatitude warm cloud than  
661 both of LWC and IWC in the midlatitude case contributes to the greater CCN-induced  
662 changes in LWC in the midlatitude warm cloud. This is as compared to either the CCN-  
663 induced changes in LWC and subsequent changes in IWC or the INP-induced changes in  
664 IWC and subsequent changes in LWC in the midlatitude case.

665       To confirm above-described mechanisms in this section, which explain different  
666 aerosol-cloud interactions between the polar and midlatitude cases, the 200\_2\_fac10 run is  
667 repeated by increasing INP by a factor of 10 in the PBL at the first time step. This repeated  
668 run is referred to as “the 200\_2\_fac10\_INP10 run. Then, the 200\_2\_fac10 run is repeated  
669 again by increasing CCN by a factor of 10 in the PBL at the first time step. This repeated  
670 run is referred to as the 200\_2\_fac10\_CCN10 run. These repeated runs are to see the  
671 response of IWC and LWC to the increasing concentration of aerosols acting as INP and  
672 CCN. This is when IWC and LWC are at the same order of magnitude and lower in mixed-

673 phase clouds than LWC in the warm-cloud counterpart as in the 200\_2\_fac10 run and  
674 midlatitude case. Comparisons between the 200\_2\_fac10, 200\_2\_fac10\_INP10 and  
675 200\_2\_fac10\_CCN10 runs show that the INP-induced changes in IWC and LWC are  
676 similar to the CCN-induced changes in IWC and LWC, respectively, as in the midlatitude  
677 case. These comparisons also show that the CCN-induced changes in LWC in the polar  
678 warm cloud are greater. This is as compared to either the CCN-induced changes in LWC  
679 and subsequent changes in IWC between the 200\_2\_fac10 and 200\_2\_fac10\_CCN10 runs  
680 or the INP-induced changes in IWC and subsequent changes in LWC between the  
681 200\_2\_fac10 and 200\_2\_fac10\_INP10 runs. These comparisons demonstrate that  
682 differences in ICNC/CDNC play a critical role in differences in aerosol-cloud interactions  
683 between the polar and midlatitude cases, considering that differences in ICNC/CDNC  
684 between the 200\_2 and 200\_2\_fac10 runs are at the same order of magnitude of those  
685 between the cases.

686

### 687 **3.3 Radiation**

688

689 Studies (e.g., Ovchinnikov et al., 2011; Possner et al., 2017; Solomon et al., 2018) have  
690 focused on radiative cooling and subsequent changes in stability and dynamics as a primary  
691 driver for the development of mixed-phase stratocumulus clouds and aerosol-induced  
692 changes in LWC and IWC in those clouds. Motivated by these studies, to isolate the role  
693 of radiative processes in cloud development and aerosol impacts on LWC and IWC, all of  
694 the simulations above are repeated by turning off radiative processes. In these repeated  
695 runs, radiative fluxes over the whole domain and simulation period are zero. The basic  
696 summary of results from these repeated runs is given in Table 3. As seen in comparisons  
697 between Tables 2 and 3, the qualitative nature of results, which are mainly about  
698 differences in IWC/LWC, the relative importance of the impacts of INP on IWC and LWC  
699 as compared to those impacts of CCN, and how warm and mixed-phase clouds are related  
700 between the polar and midlatitude cases, in this study does not vary with whether radiative  
701 processes exist or not. This demonstrates that ICNC, CDNC, deposition and condensation  
702 but not radiative processes drive results in this study.

703

## 704 4. Discussion

### 705 706 4.1 Examination of the role of ICNC/CDNC in IWC/LWC in 200\_2, 707 2000\_20, 2000\_2, 200\_20, 200\_2\_fac10, 200\_2\_fac10\_CCN10 and 708 200\_2\_fac10\_INP10 runs 709

710 So far, comparisons between the set of the 200\_2, 2000\_20, 2000\_2 and 200\_20 runs for  
711 the polar case and the other set of the 200\_2\_fac10, 200\_2\_fac10\_CCN10 and  
712 200\_2\_fac10\_INP10 runs, which represents the midlatitude case, have been mainly utilized  
713 to understand the role of ICNC/CDNC. However, even when it comes to all the runs in  
714 both the sets, differences in ICNCavg/CDNCavg and IWC/LWC are shown among them  
715 (Tables 1 and 2). For more robust examination of particularly the role of ICNC/CDNC in  
716 IWC/LWC, which is basically about the increase (decrease) in ICNC/CDNC inducing the  
717 increase (decrease) in IWC/LWC as identified from the comparison between the 200\_2 and  
718 200\_2\_fac10 runs in Section 3.1.2, all the runs in the sets are utilized by ordering them as  
719 shown in Table 4. This ordering is done in a way that as we move from the first run in the  
720 first row to the last run in the last row of Table 4, ICNCavg/CDNCavg increases. Overall,  
721 with increasing ICNCavg/CDNCavg, IWC/LWC increases, although the increase in  
722 IWC/LWC is highly non-linear in terms of the increase in ICNCavg/CDNCavg as seen in  
723 the percentage increases, and a decrease in IWC/LWC is seen with an increase in  
724 ICNCavg/CDNCavg from the 2000\_20 run to the 200\_2 run (Table 4); this high-degree  
725 non-linearity in the increase in IWC/LWC is associated with the fact that interactions  
726 between cloud microphysical, thermodynamic and dynamic processes are well known to  
727 be highly non-linear. Hence, overall, findings regarding the role of ICNC/CDNC in  
728 IWC/LWC from the comparison between the 200\_2 and 200\_2\_fac10 runs are applicable  
729 to all the runs in the sets except for the role between the 2000\_20 and 200\_2 runs. Here, it  
730 is notable that the percentage difference in ICNCavg/CDNCavg is ~9% between the  
731 2000\_20 and 200\_2 runs and the smallest among those differences in Table 4. The other  
732 differences are larger than 80%. Hence, the percentage difference in ICNCavg/CDNCavg  
733 for a pair of the 2000\_20 and 200\_2 runs is at least ~one order of magnitude smaller than  
734 that for the other pairs of the runs in Table 4. This means that findings from the comparison



735 between the 200\_2 and 200\_2\_fac10 runs are not suitable to explain the variation of  
736 IWC/LWC among clouds when the variation of ICNC/CDNC is relatively insignificant.  
737 According to Table 4, it seems that the variation of ICNC/CDNC should be greater than a  
738 critical value above which those findings are useful to account for the IWC/LWC variation  
739 among clouds.

740

#### 741 **4.2 Role of a given ICNC/CDNC in IWC/LWC for different concentrations of** 742 **aerosols acting as INP and CCN**

743

744 Simulations which are compared in Section 4.1 and shown in Table 4 have not only  
745 different ICNC<sub>avg</sub>/CDNC<sub>avg</sub> but also the different number concentrations of aerosols  
746 acting as CCN and INP at the first time step (Table 1). To better isolate particularly the  
747 role of ICNC/CDNC in IWC/LWC, we need to show that results in Section 4.1 are valid  
748 regardless of the variation of the number concentration of aerosols. For this need, we focus  
749 on the 200\_2 and 200\_2\_fac10 runs, since the primary understanding of the role of  
750 ICNC/CDNC in IWC/LWC comes from the comparison between these runs as described  
751 in Section 3.1.2. To fulfill the need, each of these runs are repeated by varying the number  
752 concentration of aerosols acting as CCN and INP in a way that ICNC<sub>avg</sub>/CDNC<sub>avg</sub> does  
753 not vary (Tables 1 and 5). The 4000\_45 and 13\_0.1 runs are the repeated 200\_2 run, and  
754 the 4000\_1.8\_fac10 and 12\_0.0035\_fac10 runs are the repeated 200\_2\_fac10 run (Tables  
755 1 and 5). The set of the 200\_2, 4000\_45 and 13\_0.1 runs is referred to as the polar set, and  
756 that of the 200\_2\_fac10, 4000\_1.8\_fac10 and 12\_0.0035\_fac10 runs is referred to as the  
757 midlatitude set in this section. Among the three runs in each of the sets, less than 4%  
758 variation of IWC/LWC is shown (Table 5). This less-than-4% variation is so small that the  
759 start contrast in IWC/LWC between the 200\_2 and 200\_2\_fac10 runs as discussed in  
760 Section 3.1.2 is also shown between the polar and midlatitude sets (Table 5). Hence, the  
761 role of the difference in a given ICNC/CDNC in the difference in IWC/LWC between the  
762 200\_2 and 200\_2\_fac10 runs as described in Section 3.1.2 is considered robust to the  
763 varying concentration of aerosols.

764

## 765 **5. Summary and conclusions**

766

767 In this study, a case of mixed-phase clouds in a polar area, which is referred to as “the polar  
768 case” is compared to that in a midlatitude area, which is referred to as “the midlatitude  
769 case”. This is to gain an understanding of how different ICNC/CDNC plays a role in  
770 making differences in cloud properties, aerosol-cloud interactions and impacts of ice  
771 processes on them between two representative areas (i.e., polar and midlatitude areas)  
772 where mixed-phase stratiform clouds form and develop. Among those cloud properties,  
773 this study focuses on IWC/LWC that plays an important role in cloud radiative properties.  
774 To gain the understanding efficiently, the polar case is chosen in a way to make stark  
775 contrast with the midlatitude case in terms of ICNC/CDNC and IWC/LWC. Although such  
776 polar cases may be uncommon, the stark contrast provides an opportunity to elucidate  
777 mechanisms that control the above-mentioned role of different ICNC/CDNC.

778 Due to lower air temperature, more ice crystals are nucleated, leading to higher  
779 ICNC/CDNC in the polar case than in the midlatitude case. This higher ICNC/CDNC  
780 enables the more efficient deposition of water vapor onto ice crystals in the polar case. This  
781 leads to much higher IWC/LWC in the polar case. The more efficient deposition of water  
782 vapor onto ice crystals enables the polar mixed-phase clouds to have the greater total cloud  
783 mass than the polar warm clouds. However, the less efficient deposition of water vapor  
784 onto ice crystals causes the midlatitude mixed-phase clouds to have less total cloud mass  
785 than the midlatitude warm clouds. With the increasing ICNC/CDNC from the midlatitude  
786 case to the polar case, impacts of CCN (IFN) on the total cloud mass become less (more)  
787 important.

788 This study picked ICNC/CDNC, which is affected by air temperature and its impacts  
789 on ice-crystal nucleation, as an important factor which differentiates IWC/LWC and  
790 interactions among clouds, aerosols and ice processes in the polar area from those in the  
791 midlatitude area. Differences in ICNC/CDNC initiate differences in the microphysical  
792 properties (e.g., the integrated surface area), and then, subsequently induce those in  
793 thermodynamic latent-heat processes (e.g., condensation and deposition), dynamics of  
794 clouds, IWC/LWC and interactions among clouds, aerosols and ice processes. However,  
795 this does not mean that no other potential factors, which can explain the variation of  
796 IWC/LWC and interactions among clouds, aerosols and ice processes between those areas,

797 exist. For example, differences in environmental factors (e.g., stability and wind shear)  
798 between the areas can have an impact on the variation. Particularly, differences in stability  
799 and wind shear can initiate those in the dynamic development of turbulence. Then, this  
800 subsequently induces differences in the microphysical and thermodynamic development of  
801 clouds, IWC/LWC and interactions among clouds, aerosols and ice processes. Hence,  
802 factors such as stability and wind shear can have different orders of procedures, which  
803 involve dynamics, thermodynamics and microphysics, than ICNC/CDNC in terms of  
804 differentiation between the polar and midlatitude mixed-phase clouds. Thus, different  
805 mechanisms controlling the differentiation can be expected regarding factors such as  
806 stability and wind shear as compared to ICNC/CDNC. The examination of these different  
807 mechanisms among stability, wind shear and ICNC/CDNC deserves future study for more  
808 comprehensive understanding of the differentiation.

809 Another point to make is that the cases in this study have weak precipitation and the  
810 associated weak sedimentation of ice crystals and droplets. In mixed-phase clouds with  
811 strong precipitation and the sedimentation, they can play roles as important as in-cloud  
812 latent-heat processes in IWC/LWC and interactions among clouds, aerosols and ice  
813 processes. In those clouds with strong precipitation, the sedimentation can take part in the  
814 interplay between ICNC/CDNC and latent-heat processes by affecting cloud mass and  
815 associated ICNC and CDNC significantly, and play a role in the differentiation of  
816 IWC/LWC and interactions among clouds, aerosols and ice processes when it comes to  
817 different cases of mixed-phase clouds. For more generalization of results here, this  
818 potential role of sedimentation needs to be investigated by performing more case studies  
819 involving cases with strong precipitation in the future.

820 It should be emphasized that although this study mentions air temperature as a factor  
821 that affects ICNC/CDNC, ICNC/CDNC can be affected by other factors such as sources of  
822 aerosols acting as INP and those acting as CCN, and/or the advection of those aerosols.  
823 Hence, even for cloud systems that develop with a similar air-temperature condition, for  
824 example, when those systems are affected by different sources of aerosols and/or their  
825 different advection, they are likely to have different ICNC/CDNC, IWC/LWC, relative  
826 importance of impacts of INP on IWC and LWC as compared to those impacts of CCN,  
827 and relation between warm and mixed-phase clouds.

828 Previous studies on mixed-phase stratocumulus clouds (e.g., Ovchinnikov et al., 2011;  
829 Possner et al., 2017; Solomon et al., 2018) have primarily focused on investigating the  
830 impacts of cloud-top radiative cooling, entrainment, and sedimentation of ice particles on  
831 these clouds, as well as their interactions with aerosols. However, there are a scarcity of  
832 studies that specifically examine the role of microphysical interactions, involving  
833 processes such as condensation and deposition, as well as factors like cloud-particle  
834 concentrations, between ice and liquid particles in mixed-phase stratocumulus clouds, and  
835 their interactions with aerosols as performed in this study. Therefore, our study contributes  
836 to a more comprehensive understanding of mixed-phase clouds and their intricate interplay  
837 with aerosols.

838 This study suggests that a microphysical factor, which is ICNC/CDNC, can be a  
839 simplified and useful tool to understand differences among different systems of  
840 stratocumulus clouds in various regions in terms of IWC/LWC and the relative importance  
841 of INP and CCN in aerosol-cloud interactions, and thus to contribute to the development  
842 of general parameterizations of those clouds in various regions for climate models. This  
843 factor can also be a useful tool for a simplified understanding of different roles of ice  
844 processes when mixed-phase clouds are compared to their warm-cloud counterparts in  
845 terms of the cloud development and its interactions with aerosols among those different  
846 systems. It should be noted that warm clouds have been studied much more than mixed-  
847 phase clouds, although mixed-phase clouds play as important roles as warm clouds in the  
848 evolution of climate and its change. This study provides preliminary mechanisms which  
849 differentiate mixed-phase clouds and their interactions with aerosols from their warm-  
850 cloud counterparts, and control the variation of the differentiation in different regions as a  
851 way of improving our understanding of mixed-phase clouds. It should be mentioned that  
852 the efficient way of developing general parameterizations, which are for climate models  
853 and consider all of warm, mixed-phase clouds in various regions and their interactions with  
854 aerosols, can be achieved by just adding those mechanisms to pre-existing  
855 parameterizations of much-studied warm clouds instead of developing brand new  
856 parameterizations from the scratch. Hence, although those mechanisms identified in this  
857 study may not be complete, they can act as a valuable building block that can streamline  
858 the development of those general parameterizations.

859 **Code/Data source and availability**

860

861 Our private computer system stores the code/data which are private and used in this study.  
862 Upon approval from funding sources, the data will be opened to the public. Projects related  
863 to this paper have not been finished, thus, the sources prevent the data from being open to  
864 the public currently. However, if information on the data is needed, contact the  
865 corresponding author Seoung Soo Lee (slee1247@umd.edu).

866

867 **Author contributions**

868 Essential initiative ideas are provided by SSL, CHJ and YJY to start this work. Simulation  
869 and observation data are analyzed by SSL, CHJ and JU. YZ, JP, MGM and SKS review  
870 the results and contribute to their improvement. JC provides supports to set up and run  
871 additional simulations during the review.

872

873 **Competing interests**

874 The authors declare that they have no conflict of interest.

875

876 **Acknowledgements**

877 This study is supported by the National Research Foundation of Korea (NRF) grant funded  
878 by the Korea government (MSIT) (Nos. NRF2020R1A2C1003215,  
879 NRF2020R1A2C2011081, NRF2023R1A2C1002367,  
880 NRF2021M1A5A1065672/KOPRI-PN23011 and 2020R1A2C1013278), and Basic  
881 Science Research Program through the NRF funded by the Ministry of Education (No.  
882 2020R1A6A1A03044834).

883

884

885

886

887

888

889

890

891

892 **References**

893

894 Ackerman, A., Kirkpatrick, M., Stevens, D., et al.: The impact of humidity above  
895 stratiform clouds on indirect aerosol climate forcing, *Science*, 432, 1014–1017,  
896 <https://doi.org/10.1038/nature03174>, 2004.

897 Albrecht, B. A.: Aerosols, cloud microphysics, and fractional cloudiness, *Science*, 245,  
898 1227–1230, 1989.

899 Bartosiewicz, Y., and Duponcheel, M.: Large eddy simulation: Application to liquid metal  
900 fluid flow and heat transfer . In: Roelofs, Ferry, *Thermal Hydraulics Aspects of Liquid*  
901 *Metal Cooled Nuclear Reactors*, Woodhead Publishing, 2018.

902 Brown, A., Milton, S., Cullen, M., Golding, B., Mitchell, J., and Shelly, A.: Unified  
903 modeling and prediction of weather and climate: A 25-year journey, *B. Am. Meteorol.*  
904 *Soc.*, 93, 1865–1877, 2012.

905 Chen, F., and Dudhia, J.: Coupling an advanced land-surface hydrology model with the  
906 Penn State-NCAR MM5 modeling system. Part I: Model description and  
907 implementation, *Mon. Wea. Rev.*, 129, 569–585, 2001.

908 Choi, Y.-S., Ho, C.-H., Park, C.-E., Storelvmo, T., and Tan, I.: Influence of cloud phase  
909 composition on climate feedbacks, *J. Geophys. Res.*, 119, 3687–3700,  
910 doi:10.1002/2013JD020582, 2014.

911 Choi, Y.-S., Lindzen, R. S., Ho, C.-H., and Kim, J.: Space observations of cold-cloud phase  
912 change, *Proc. Natl. Acad. Sci. U.S.A.*, 107, 11211–11216, 2010

913 Chua, X. R., and Ming, Y.: Convective invigoration traced to warm-rain microphysics,  
914 *Geophys. Res. Lett*, 47, <https://doi.org/10.1029/2020GL089134>, 2020.

915 Dione, C., Lohou, F., Lothon, M., Adler, B., Babić, K., Kalthoff, N., Pedruzo-Bagazgoitia,  
916 X., Bezombes, Y., and Gabella, O.: Low-level stratiform clouds and dynamical  
917 features observed within the southern West African monsoon, *Atmos. Chem. Phys.*,  
918 19, 8979–8997, <https://doi.org/10.5194/acp-19-8979-2019>, 2019.

919 Donovan, D. P., Ice-cloud effective particle size parameterization based on combined lidar,  
920 radar reflectivity, and mean Doppler velocity measurements, *J. Geophys. Res.*, 108,  
921 4573, doi:10.1029/2003JD003469, 2003.

922 Donovan, D. P., van Lammeren, A.C.A.P. , Hogan, R. J., Russchenberg, H. W. J., Apituley,

- 923 A., Francis, P., Testud, J., Pelon, J., Quante, M., and Goddard, J. W. F.: Cloud effective  
924 particle size and water content profile retrievals using combined lidar and radar  
925 observations – 2. Comparison with IR radiometer and in situ measurements of ice  
926 clouds, *J. Geophys. Res.*, 106, 27449-27464, 2001.
- 927 Dudhia, J., Numerical study of convection observed during the winter monsoon  
928 Experiment using a mesoscale two-dimensional Model, *J. Atmos. Sci.*, 46, 3077–3107,  
929 <https://doi.org/10.1175/1520-0469>, 1989.
- 930 Fan, J., Rosenfeld, D., Zhang, Y., Giangrande, S. E., Li, Z., Machado, L. A. T., Martin, S.  
931 T., Yang, Y., Wang, J., and Artaxo, P.: Substantial convection and precipitation  
932 enhancements by ultrafine aerosol particles. *Science*, 359, 411–418, 2018
- 933 Forster, P., et al., Changes in atmospheric constituents and in radiative forcing, in: *Climate*  
934 *change 2007: the physical science basis*, Contribution of working group I to the Fourth  
935 Assessment Report of the Intergovernmental Panel on Climate Change, edited by  
936 Solomon, S., et al., Cambridge Univ. Press, New York, 2007.
- 937 Hahn, C. J., and Warren, S. G.: A gridded climatology of clouds over land (1971–96) and  
938 ocean (1954–97) from surface observations worldwide, Numeric Data Package NDP-  
939 026EORNL/CDIAC-153, CDIAC, Department of Energy, Oak Ridge, TN, 2007.
- 940 Hannak, L., Knippertz, P., Fink, A. H., Kniffka, A., and Pante, G.: Why do global climate  
941 models struggle to represent low-level clouds in the West African summer monsoon?,  
942 *J. Climate*, 30, 1665–1687, <https://doi.org/10.1175/JCLI-D-16-0451.1>, 2017
- 943 Hartmann, D. L., Ockert-Bell, M. E., and Michelsen, M. L.: The effect of cloud type on  
944 earth’s energy balance—Global analysis, *J. Climate*, 5, 1281–1304, 1992.
- 945 Hartmann, M., Gong, X., Kecorius, S., van Pinxteren, M., Vogl, T., Welti, A., Wex, H.,  
946 Zeppenfeld, S., Herrmann, H., Wiedensohler, A., and Stratmann, F.: Terrestrial or  
947 marine – indications towards the origin of ice-nucleating particles during melt season  
948 in the European Arctic up to 83.7° N, *Atmos. Chem. Phys.*, 21, 11613–11636,  
949 <https://doi.org/10.5194/acp-21-11613-2021>, 2021.
- 950 Hogan, R. J., Illingworth, A. J., O’Connor, E. J., et al.: Cloudnet: Evaluation of model  
951 clouds using ground-based observations, ECMWF Workshop on parametrization of  
952 clouds on large-scale models., 2006.
- 953 IPCC: *Climate Change: The Physical Science Basis*. Contribution of Working Group I to

- 954 the Sixth Assessment Report of the Intergovernmental Panel on Climate Change  
955 [Masson-Delmotte, V., Zhai, P., Pirani, A., Connors, S. L., Péan, C., Berger, S., Caud,  
956 N., Chen, Y., Goldfarb, L., Gomis, M. I., Huang, M., Leitzell, K., Lonnoy, E.,  
957 Matthews, J. B. R., Maycock, T. K., Waterfield, T., Yelekçi, O., Yu, R., and Zhou, B.  
958 (eds.)]. Cambridge University Press, Cambridge, United Kingdom and New York, NY,  
959 USA, In press, doi:10.1017/9781009157896, 2021.
- 960 Jung, C. H., Yoon, Y. J., Kang, H. J., Gim, Y., Lee, B. Y., Ström, J., Krejci, R., and Tunved,  
961 P.: The seasonal characteristics of cloud condensation nuclei (CCN) in the arctic lower  
962 troposphere, *Tellus B: Chemical and Physical Meteorology*, 70:1, 1513291, [https://doi:  
963 10.1080/16000889.2018.1513291](https://doi.org/10.1080/16000889.2018.1513291), 2018.
- 964 Khain, A. P., Ovchinnikov, M., Pinsky, M., Pokrovsky, A. and Krugliak, H.: Notes on the  
965 state-of-the-art numerical modeling of cloud microphysics, *Atmos. Res.*, 55, 159–224,  
966 2000.
- 967 Khain, A., Pokrovsky, A., Rosenfeld, D., Blahak, U., and Ryzhkoy, A.: The role of CCN in  
968 precipitation and hail in a mid-latitude storm as seen in simulations using a spectral  
969 (bin) microphysics model in a 2D dynamic frame, *Atmos. Res.*, 99, 129–146, 2011.
- 970 Khain, A. P., Phillips, V., Benmoshe, N., Pokrovsky, A.: The role of small soluble aerosols  
971 in the microphysics of deep maritime clouds, *J. Atmos. Sci.*, 69, 2787–2807, 2012.
- 972 Knippertz, P., Fink, A. H., Schuster, R., Trentmann, J., Schrage, J. M., and Yorke, C.: Ultra-  
973 low clouds over the southern West African monsoon region, *Geophys. Res. Lett.*, 38,  
974 L21808, <https://doi.org/10.1029/2011GL049278>, 2011.
- 975 Kogan, Y., 2013: A cumulus cloud microphysics parameterization for cloud-resolving  
976 models, *J. Atmos. Sci.*, 70, 1423–1436, [https://doi:10.1175/JAS-D-12-0183.1](https://doi.org/10.1175/JAS-D-12-0183.1), 2013.
- 977 Koop, T., Luo, B. P., Tsias, A., and Peter, T.: Water activity as the determinant for  
978 homogeneous ice nucleation in aqueous solutions, *Nature*, 406, 611-614.
- 979 Lee, H., and Baik, J.-J.: A physically based autoconversion parameterization, *J. Atmos. Sci.*,  
980 74, 1599-1616, <https://doi.org/10.1175/JAS-D-16-0207.1>, 2017.
- 981 Lee S. S., Penner, J. E., and Saleeby, S. M.: Aerosol effects on liquid-water path of thin  
982 stratocumulus clouds, *J. Geophys. Res.*, 114, D07204, doi:10.1029/2008JD010513,  
983 2009.
- 984 Lee, S. S., et al., Mid-latitude mixed-phase stratocumulus clouds and their interactions with



- 985 aerosols: how ice processes affect microphysical, dynamic and thermodynamic  
986 development in those clouds and interactions?, *Atmos. Chem. Phys.*,  
987 <https://doi.org/10.5194/acp-21-16843-2021>, 2022.
- 988 Li, J., Carlson, B. E., Yung, Y. L., Lv, D., Hansen, J., Penner, J. E., Liao, H., Ramaswamy,  
989 V., Kahn, R. A., Zhang, P., Dubovik, O., Ding, A., Lacis, A. A., Zhang, L., and Dong,  
990 Y.: Scattering and absorbing aerosols in the climate system, *Nature Reviews Earth and*  
991 *Environment*, 3, 363–379, <https://doi.org/10.1038/s43017-022-00296-7>, 2022.
- 992 Lilly, D. K.: The representation of small scale turbulence in numerical simulation  
993 experiments, *Proc. Ibm Sci. Comput. Symp. Environ. Sci.*, 320–1951, 195–210, 1967.
- 994 Lim, K.-S. S., and Hong, S.-Y.: Development of an effective double-moment cloud  
995 microphysics scheme with prognostic cloud condensation nuclei (CCN) for weather  
996 and climate models, *Mon. Wea. Rev.*, 138, 1587–1612,  
997 doi:10.1175/2009MWR2968.1., 2010.
- 998 Liu, Y., and Daum, P. H.: Parameterization of the autoconversion. Part I: Analytical  
999 formulation of the Kessler-type parameterizations, *J. Atmos. Sci.*, 61, 1539–1548,  
1000 doi:10.1175/1520-0469(2004)061,1539:POTAPI.2.0.CO;2, 2004.
- 1001 Lohmann, U. and Diehl, K.: Sensitivity studies of the importance of dust ice nuclei for  
1002 the indirect aerosol effect on stratiform mixed-phase clouds, *J. Atmos. Sci.*, 63, 968-  
1003 982, 2006.
- 1004 Mansell, E. R., Ziegler, C. L. and Bruning, E. C., Simulated electrification of a small  
1005 thunderstorm with two-moment bulk microphysics, *J. Atmos. Sci.*, 67, 171–194,  
1006 doi:10.1175/2009JAS2965.1., 2010.
- 1007 Ming, Y., and Chua, X. R.: Convective invigoration traced to warm-rain microphysics,  
1008 *Geophys. Res. Lett.*, 47, doi.org/10.1029/2020GL089134, 2020.
- 1009 Mlawer, E. J., Taubman, S. J., Brown, P. D., Iacono, M. J., and Clough, S. A.: RRTM, a  
1010 validated correlated-k model for the longwave, *J. Geophys. Res.*, 102, 16663-16668,  
1011 1997.
- 1012 Möhler, O., et al, Efficiency of the deposition mode ice nucleation on mineral dust particles,  
1013 *Atmos. Chem. Phys.*, 6, 3007-3021, 2006.
- 1014 Ovchinnikov, M., Korolev, A., and Fan, J.: Effects of ice number concentration on  
1015 dynamics of a shallow mixed-phase stratiform cloud, *J. Geophys. Res.*, 116, D00T06,

- 1016 doi:10.1029/2011JD015888, 2011.
- 1017 Possner, A., Ekman, A. M. L., and Lohmann, U.: Cloud response and feedback processes  
1018 in stratiform mixed-phase clouds perturbed by ship exhaust, *Geophys. Res. Lett.*, 44,  
1019 1964–1972, <https://doi.org/10.1002/2016GL071358>, 2017.
- 1020 Pruppacher, H. R. and Klett, J. D.: *Microphysics of clouds and precipitation*, 714pp, D.  
1021 Reidel, 1978.
- 1022 Ramaswamy, V., et al.: Radiative forcing of climate change, in *Climate Change 2001: The*  
1023 *Scientific Basis*, edited by J. T. Houghton et al., 349-416, Cambridge Univ. Press,  
1024 New York, 2001.
- 1025 Solomon, A., de Boer, G., Creamean, J. M., McComiskey, A., Shupe, M. D., Maahn, M.,  
1026 and Cox, C.: The relative impact of cloud condensation nuclei and ice nucleating  
1027 particle concentrations on phase partitioning in Arctic mixed-phase stratocumulus  
1028 clouds, *Atmos. Chem. Phys.*, 18, 17047–17059, [https://doi.org/10.5194/acp-18-](https://doi.org/10.5194/acp-18-17047-2018)  
1029 [17047-2018](https://doi.org/10.5194/acp-18-17047-2018), 2018.
- 1030 Smagorinsky, J.: General circulation experiments with the primitive equations, *Mon. Wea.*  
1031 *Rev.*, 91, 99–164, 1963.
- 1032 Stevens, B., and Feingold, G.: Untangling aerosol effects on clouds and precipitation in a  
1033 buffered system, *Nature*, 461, 607–613, <https://doi.org/10.1038/nature08281>, 2009.
- 1034 Stephens, G. L., and Greenwald, T. J.: Observations of the Earth’s radiation budget in  
1035 relation to atmospheric hydrology. Part II: Cloud effects and cloud feedback, *J.*  
1036 *Geophys. Res.*, 96, 15 325–15 340, 1991.
- 1037 Tinel, C., Testud, J., Hogan, R. J., Protat, A., Delanoe, J. and Bouniol, D.: The retrieval of  
1038 ice cloud properties from cloud radar and lidar synergy, *J. Appl. Meteorol.*, 44, 860-  
1039 875, 2005.
- 1040 Tunved, P., Ström, J. and Krejci, R.: Arctic aerosol life cycle: linking aerosol size  
1041 distributions observed between 2000 and 2010 with air mass transport and  
1042 precipitation at Zeppelin station, Ny-Ålesund, Svalbard, *Atmos. Chem. Phys.*,  
1043 13, 3643–3660, <https://doi.org/10.5194/acp-13-3643-2013>, 2013
- 1044 Twomey, S.: Pollution and the Planetary Albedo, *Atmos. Env.*, 8, 1251-1256, 1974.
- 1045 Warren, S. G., Hahn, C. J., London, J., Chervin, R. M., and Jenne, R. L.: Global distribution  
1046 of total cloud cover and cloud types over land, NCAR Tech. Note NCAR/TN-

1047 273+STR, National Center for Atmospheric Research, Boulder, CO, 29 pp. + 200  
1048 maps, 1986.

1049 Wood, R.: Stratocumulus clouds, *Mon. Wea. Rev.*, 140, 2373-2423, 2012.

1050 Zhang, D., Vogelmann, A., Kollias, P., Luke, E., Yang, F., Lubin, D., and Wang, Z.:  
1051 Comparison of Antarctic and Arctic single-layer stratiform mixed-phase cloud  
1052 properties using ground-based remote sensing measurements, *J. Geophys. Res.*, 124,  
1053 10186–10204, <https://doi.org/10.1029/2019JD030673>, 2019.

1054 Zheng, Y., Zhang, H., Rosenfeld, D., Lee, S. S., Su, T., and Li, Z.: Idealized Large-Eddy  
1055 Simulations of Stratocumulus Advecting over Cold Water. Part I: Boundary Layer  
1056 Decoupling, 78, 4089-4102, <https://doi.org/10.1175/JAS-D-21-0108.1>, 2021.

1057

1058

1059

1060

1061

1062

1063

1064

1065

1066

1067

1068

1069

1070

1071

1072

1073

1074

1075

1076

1077

1078

1079

1080

1081

1082

1083

1084

1085

1086

1087

1088 **FIGURE CAPTIONS**

1089

1090 Figure 1. A red rectangle marks the simulation domain in the Svalbard area, Norway. The  
1091 light blue represents the ocean and the green the land area.

1092

1093 Figure 2. (a) The vertical distributions of the domain-averaged potential temperature and  
1094 humidity at the first time step, (b) the time series of the domain-averaged large-scale  
1095 subsidence or downdraft at the model top and (c) the time series of the domain-averaged  
1096 surface temperature.

1097

1098 Figure 3. Aerosol size distribution at the surface.  $N$  represents aerosol number  
1099 concentration per unit volume of air and  $D$  represents aerosol diameter.

1100

1101 Figure 4. The vertical distributions of the time- and domain-averaged IWC and LWC in  
1102 the 200\_2 and 200\_2\_noice runs.

1103

1104 Figure 5. The vertical distributions of the time- and domain-averaged deposition and  
1105 condensation rates in the 200\_2 and 200\_2\_noice runs.

1106

1107 Figure 6. The vertical distributions of the time- and domain-averaged IWC and LWC in  
1108 the 200\_2, 200\_2\_noice and 200\_2\_fac10 runs.

1109

1110 Figure 7. The vertical distributions of the time- and domain-averaged (a) IWC in the 200\_2,  
1111 2000\_20, 200\_2\_fac10, 200\_20, 2000\_2, 200\_2\_fac10\_CCN10, and 200\_2\_fac10\_INP10  
1112 runs. (b) The vertical distributions of the time- and domain-averaged LWC in the  
1113 200\_2\_noice and 2000\_2\_noice runs as well as all the runs shown in panel (a),.

1114

1115

1116

1117

1118

Simulations	The number concentration of aerosols acting as CCN at the first time step in the PBL ( $\text{cm}^{-3}$ )	The number concentration of aerosols acting as INP at the first time step in the PBL ( $\text{cm}^{-3}$ )	ICNCavg/CDNCavg	Ice processes	Radiation
200 2	200	2	0.220	Present	Present
2000 20	2000	20	0.201	Present	Present
2000 2	2000	2	0.108	Present	Present
200 20	200	20	0.512	Present	Present
200 2 noice	200	2	0.000	Absent	Present
2000 2 noice	2000	2	0.000	Absent	Present
200 2 fac10	200	0.07	0.022	Present	Present
200 2 fac10 CCN10	2000	0.07	0.012	Present	Present
200 2 fac10 INP10	200	0.7	0.041	Present	Present
200 2 norad	200	2	0.218	Present	Absent
2000 20 norad	2000	20	0.197	Present	Absent
2000 2 norad	2000	2	0.101	Present	Absent
200 20 norad	200	20	0.502	Present	Absent
200 2 noice norad	200	2	0.000	Absent	Absent
2000 2 noice norad	2000	2	0.000	Absent	Absent
200 2 fac10 norad	200	0.07	0.022	Present	Absent
200 2 fac10 CCN10 norad	2000	0.07	0.010	Present	Absent
200 2 fac10 INP10 norad	200	0.7	0.038	Present	Absent
4000 45	4000	45	0.220	Present	Present
13 0.1	13	0.1	0.220	Present	Present
4000 1.8 fac10	4000	1.8	0.022	Present	Present
12 0.0035 fac10	12	0.0035	0.022	Present	Present

1119

1120 Table 1. Summary of simulations

1121

1122

1123

1124

1125

1126

1127

1128

1129

1130

Simulations	IWC ( $10^{-3}$ $\text{g m}^{-3}$ )	LWC ( $10^{-3}$ $\text{g m}^{-3}$ )	IWP ( $\text{g m}^{-2}$ )	LWP ( $\text{g m}^{-2}$ )	IWC/LWC	IWP/LWP	Condensation rate		Deposition rate		Cloud-base sedimentation ( $10^{-3}$ $\text{g m}^{-2} \text{s}^{-1}$ )		Entrainment ( $\text{cm s}^{-1}$ )
							Over grid points ( $10^{-2}$ $\text{g m}^{-3}$ $\text{s}^{-1}$ )	Over cloudy columns ( $\text{g m}^{-2}$ $\text{s}^{-1}$ )	Over grid points ( $10^{-2}$ $\text{g m}^{-3}$ $\text{s}^{-1}$ )	Over cloudy columns ( $\text{g m}^{-2}$ $\text{s}^{-1}$ )	Ice- crystal	Droplet	
200 2	6.57	0.25	31.94	1.23	26.28	25.96	0.11	1.98	1.30	23.40	1.17	0.17	0.25
2000 20	7.82	0.21	40.91	1.08	37.24	37.91	0.09	1.62	1.57	28.26	0.94	0.06	0.53
2000 2	6.55	0.29	31.85	1.46	22.58	21.81	0.12	2.16	1.28	23.04	1.11	0.08	0.28
200 20	7.80	0.20	40.82	1.01	39.00	40.42	0.09	1.62	1.56	28.08	0.97	0.11	0.51
200 2 noice	0.00	2.06	0.00	10.35	0.00	0.00	0.72	12.48	0.00	0.00	0.00	0.36	0.08
2000 2 noice	0.00	2.25	0.00	11.29	0.00	0.00	0.76	12.80	0.00	0.00	0.00	0.14	0.10
200 2 fac10	0.89	0.85	4.27	4.20	1.05	1.02	0.32	5.76	0.35	6.30	0.19	0.28	0.06
200 2 fac10 CCN10	0.79	0.97	3.82	4.83	0.81	0.79	0.38	6.84	0.31	5.58	0.17	0.19	0.07
200 2 fac10 INP10	0.98	0.78	4.73	3.88	1.25	1.22	0.31	5.58	0.39	7.02	0.14	0.22	0.07

1131

1132 Table 2. The averaged IWC, LWC, IWP, LWP, condensation and deposition rates over all  
1133 of grid points and the simulation period in each of simulations. IWC/LWC (IWP/LWP) is  
1134 the averaged IWC (IWP) over the averaged LWC (LWP). Also, as shown are the vertically  
1135 integrated condensation and deposition rates over each cloudy column which are averaged  
1136 over those columns and the simulation period. The average cloud-base sedimentation rate,  
1137 which is for each of ice crystals and droplets, over the cloud base and simulation period,  
1138 and the average cloud-top entrainment rate over the cloud top and simulation period are  
1139 shown as well.

1140

1141

1142

1143

1144

1145

1146

1147

1148

1149

1150

1151

1152

1153

Simulations	IWC ( $10^{-3}$ $\text{g m}^{-3}$ )	LWC ( $10^{-3}$ $\text{g m}^{-3}$ )	IWP ( $\text{g m}^{-2}$ )	LWP ( $\text{g m}^{-2}$ )	IWC/LWC	IWP/LWP	Condensation rate		Deposition rate		Cloud-base sedimentation ( $10^{-3} \text{g m}^{-2} \text{s}^{-1}$ )		Entrainment ( $\text{cm s}^{-1}$ )
							Over grid points ( $10^{-2}$ $\text{g m}^{-3}$ $\text{s}^{-1}$ )	Over cloudy columns ( $\text{g m}^{-2}$ $\text{s}^{-1}$ )	Over grid points ( $10^{-2}$ $\text{g m}^{-3}$ $\text{s}^{-1}$ )	Over cloudy columns ( $\text{g m}^{-2}$ $\text{s}^{-1}$ )	Ice- crystal	Droplet	
200 2 norad	6.42	0.24	31.21	1.22	26.75	25.58	0.10	1.96	1.29	23.35	1.16	0.16	0.24
2000 20 norad	7.63	0.21	40.05	1.07	36.33	37.42	0.09	1.59	1.55	29.91	0.92	0.06	0.51
2000 2 norad	6.40	0.29	31.11	1.45	22.06	21.45	0.11	2.12	1.26	22.69	1.07	0.08	0.27
200 20 norad	7.61	0.20	39.95	0.99	38.05	40.35	0.09	1.59	1.54	27.72	0.97	0.11	0.49
200 2 noice norad	0.00	2.03	0.00	10.20	0.00	0.00	0.72	12.31	0.00	0.00	0.00	0.34	0.08
2000 2 noice norad	0.00	2.21	0.00	11.12	0.00	0.00	0.75	12.63	0.00	0.00	0.00	0.13	0.10
200 2 fac10 norad	0.87	0.84	4.21	4.17	1.04	1.01	0.31	5.74	0.35	6.21	0.18	0.27	0.05
200 2 fac10 CCN10 norad	0.78	0.96	3.78	4.80	0.81	0.79	0.36	6.81	0.30	5.50	0.16	0.18	0.06
200 2 fac10 INP10 norad	0.97	0.76	4.70	3.85	1.25	1.22	0.30	5.55	0.38	6.91	0.13	0.21	0.06

1154

1155 Table 3. Same as Table 2 but for the repeated simulations with radiative processes turned

1156 off.

1157

1158

1159

1160

1161

1162

1163

1164

1165

1166

1167

1168

1169

1170

1171

1172

1173

1174

1175

1176

Simulations	ICNCavg/CDNCavg	Percentage increases (+) or decrease (-) in ICNCavg/CDNCavg	IWC/LWC	Percentage increases (+) or decrease (-) in IWC/LWC
200 2 fac10 CCN10	0.012		0.81	
200 2 fac10	0.022	+83.33%	1.05	+29.6%
200 2 fac10 INP10	0.041	+86.36%	1.25	+19.0%
2000 2	0.108	+163.4%	22.58	+1706.4%
2000 20	0.201	+86.1%	37.24	+64.9%
200 2	0.220	+9.4%	26.28	-29.4%
200 20	0.512	+132.7%	39.00	+48.4%

1177

1178 Table 4. ICNCavg/CDNCavg and IWC/LWC in the simulations that are related to Section  
1179 4.1. The Percentage increases or decreases in ICNCavg/CDNCavg and IWC/LWC in the

1180  $i^{\text{th}}$  row are  $\frac{(ICNCavg/CDNCavg)_{i+1} - (ICNCavg/CDNCavg)_i}{(ICNCavg/CDNCavg)_i} \times 100 (\%)$  and

1181  $\frac{(IWC/LWC)_{i+1} - (IWC/LWC)_i}{(IWC/LWC)_i} \times 100 (\%)$ , respectively. Here,  $(ICNCavg/CDNCavg)_i$  and

1182  $(IWC/LWC)_i$  represent ICNCavg/CDNCavg and IWC/LWC in the  $i^{\text{th}}$  row, respectively.

1183

1184

1185

1186

1187

1188

1189

1190

1191

1192

1193

1194

1195

1196

1197

1198

1199

1200



Simulations	ICNCavg/CDNCavg	IWC/LWC	Percentage increases (+) or decrease (-) in IWC/LWC
Polar case			
200_2	0.220	26.28	
4000_45	0.220	27.25	+3.7%
13_0.1	0.220	25.62	-2.5%
Representing midlatitude case			
200_2_fac10	0.022	1.05	
4000_1.8_fac10	0.022	1.09	+3.8%
12_0.0035_fac10	0.022	1.02	-2.9%

1201

1202 Table 5. ICNCavg/CDNCavg and IWC/LWC in the simulations that are related to Section  
 1203 4.2. The percentage increases or decreases in IWC/LWC in the 4000\_45 run or in the

1204 13\_0.1 run are  $\frac{(IWC/LWC)_{4000\_45 \text{ or } 13\_0.1} - (IWC/LWC)_{200\_2}}{(IWC/LWC)_{200\_2}} \times 100 (\%)$ . Here,

1205  $(IWC/LWC)_{4000\_45 \text{ or } 13\_0.1}$  represents IWC/LWC in the 4000\_45 run or the 13\_01 run, while  
 1206  $(IWC/LWC)_{200\_2}$  represents IWC/LWC in the 200\_2 run. The percentage increases or

1207 decreases in IWC/LWC in the 4000\_1.8\_fac10 run or the 12\_0.0035\_fac10 run are

1208  $\frac{(IWC/LWC)_{4000\_1.8\_fac10 \text{ or } 12\_0.0035\_fac10} - (IWC/LWC)_{200\_2\_fac10}}{(IWC/LWC)_{200\_2\_fac10}} \times 100 (\%)$ . Here,

1209  $(IWC/LWC)_{4000\_1.8\_fac10 \text{ or } 12\_0.0035\_fac10}$  represents IWC/LWC in the 4000\_1.8\_fac10 run or  
 1210 the 12\_0.0035\_fac10 run, while  $(IWC/LWC)_{200\_2\_fac10}$  represents IWC/LWC in the  
 1211 200\_2\_fac10 run.

1212

1213

1214

1215

1216

1217

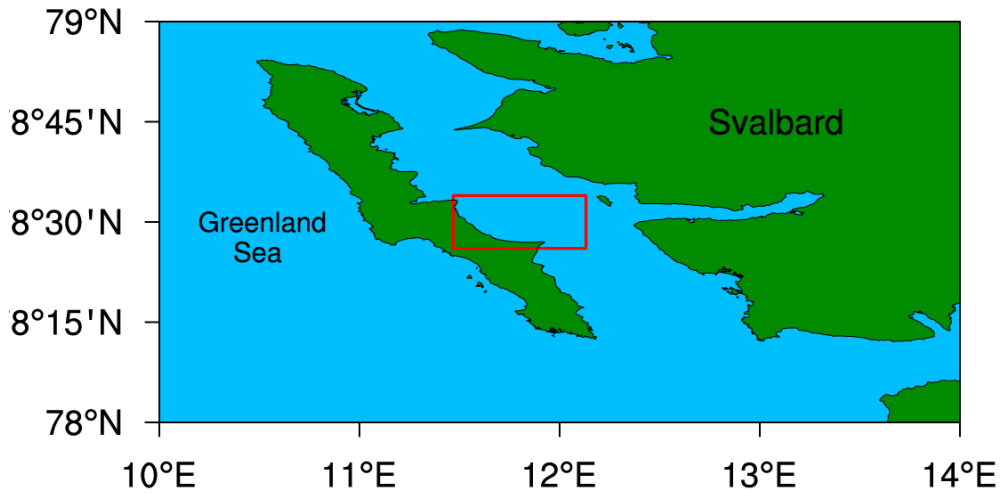
1218

1219

1220

1221

1222



1223

1224

**Figure 1**

1225

1226

1227

1228

1229

1230

1231

1232

1233

1234

1235

1236

1237

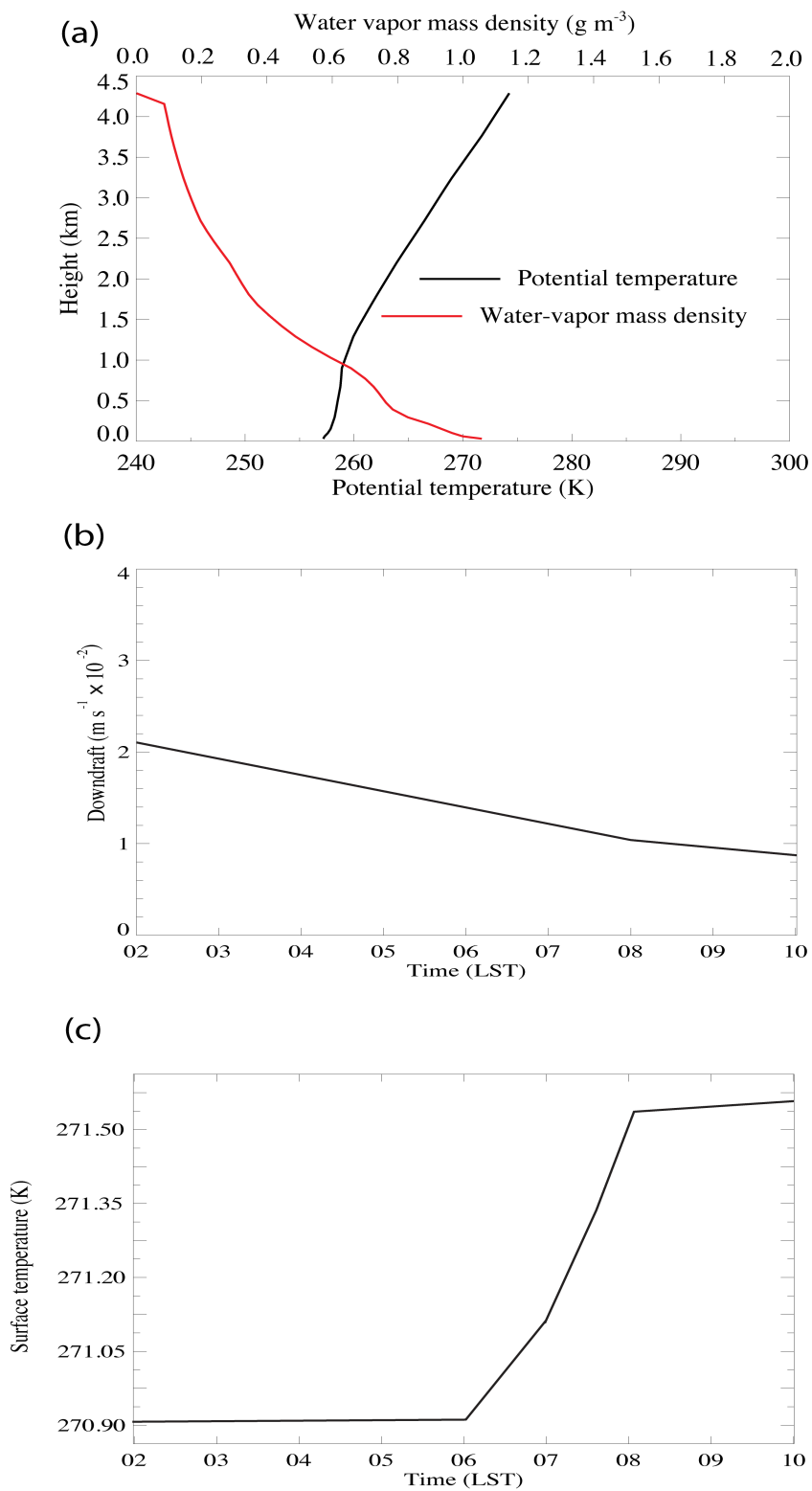
1238

1239

1240

1241

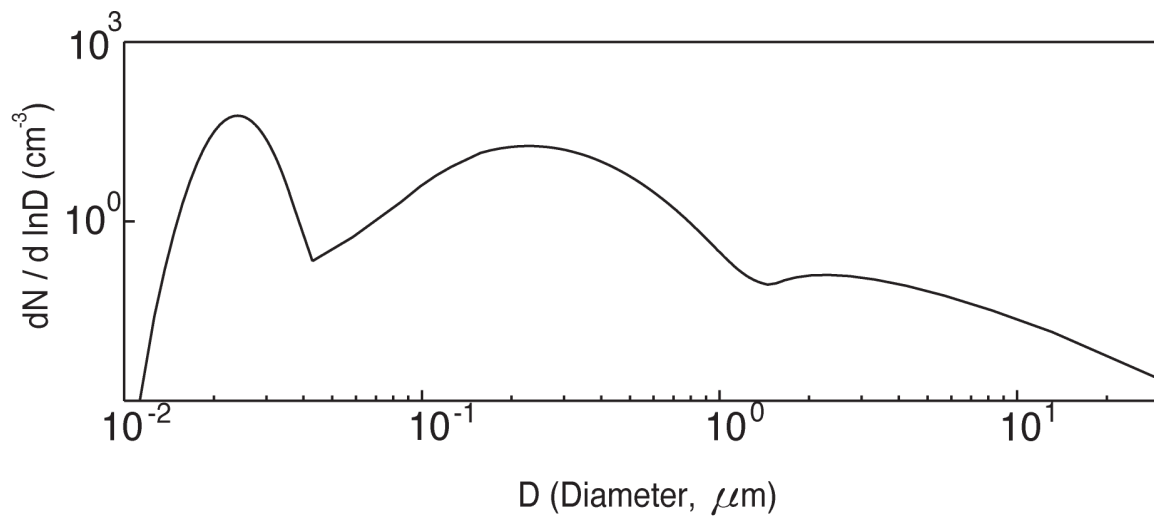
1242



1243

1244

**Figure 2**



1245

1246

**Figure 3**

1247

1248

1249

1250

1251

1252

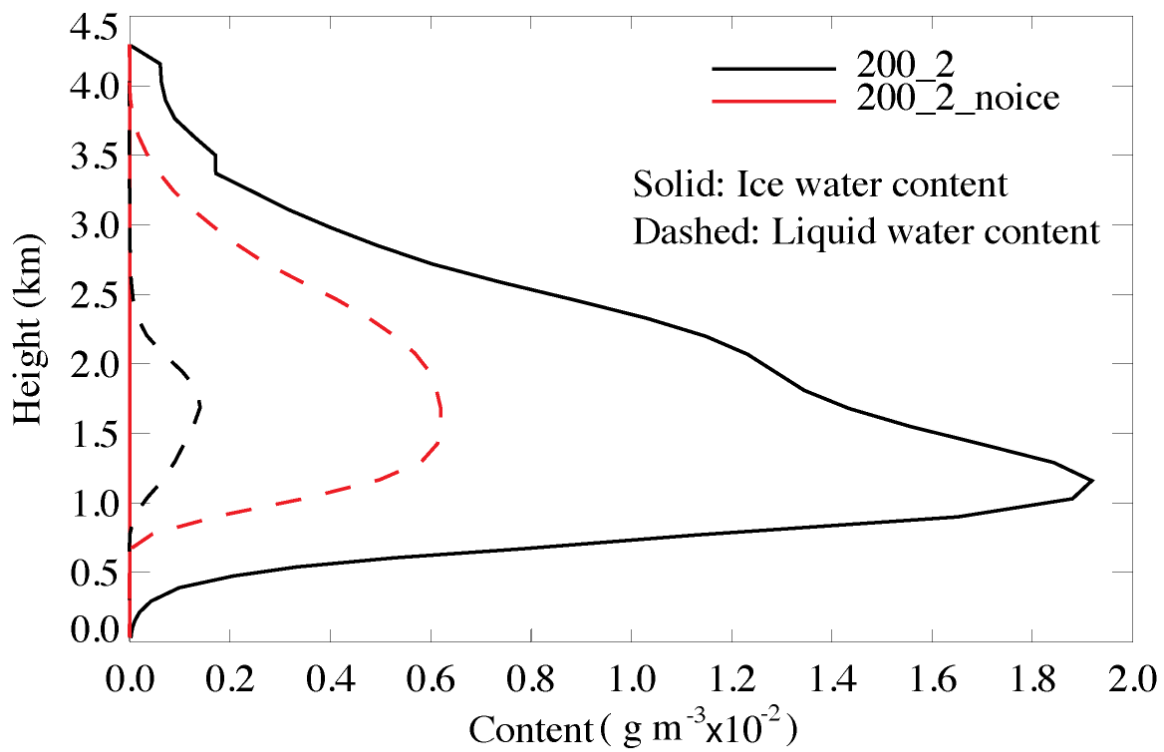
1253

1254

1255

1256

1257



1258

1259

**Figure 4**

1260

1261

1262

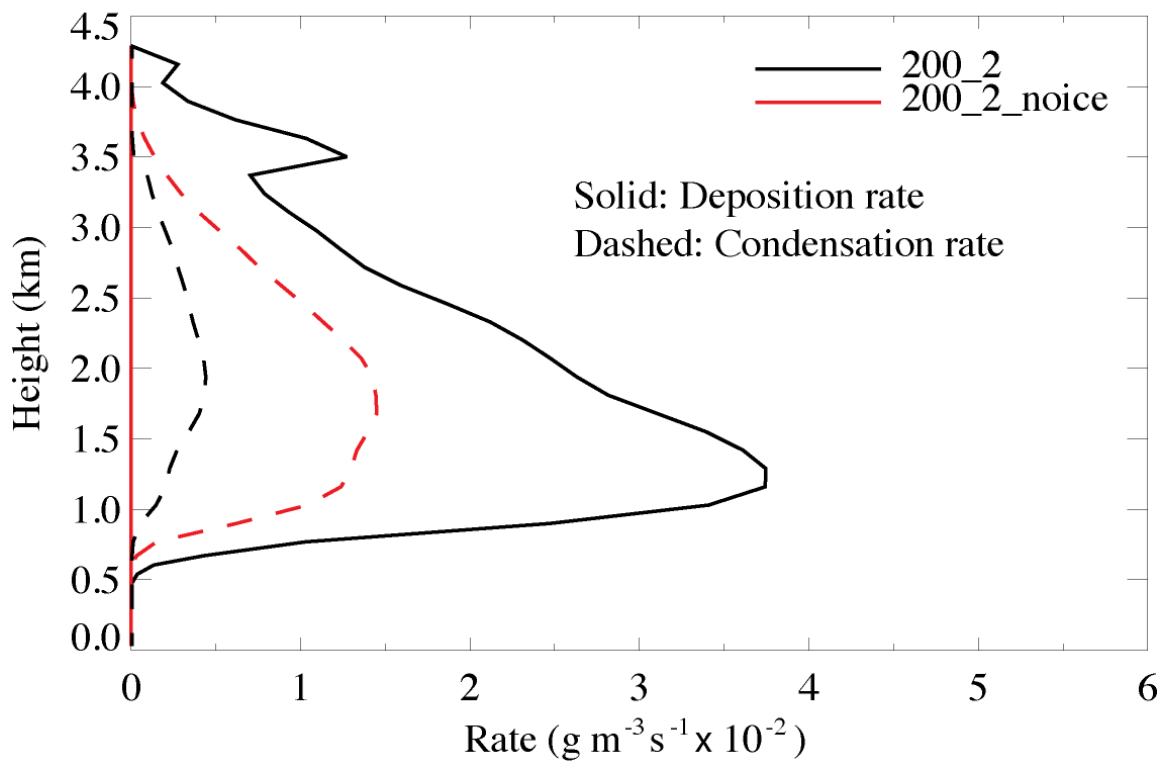
1263

1264

1265

1266

1267



1268

1269

**Figure 5**

1270

1271

1272

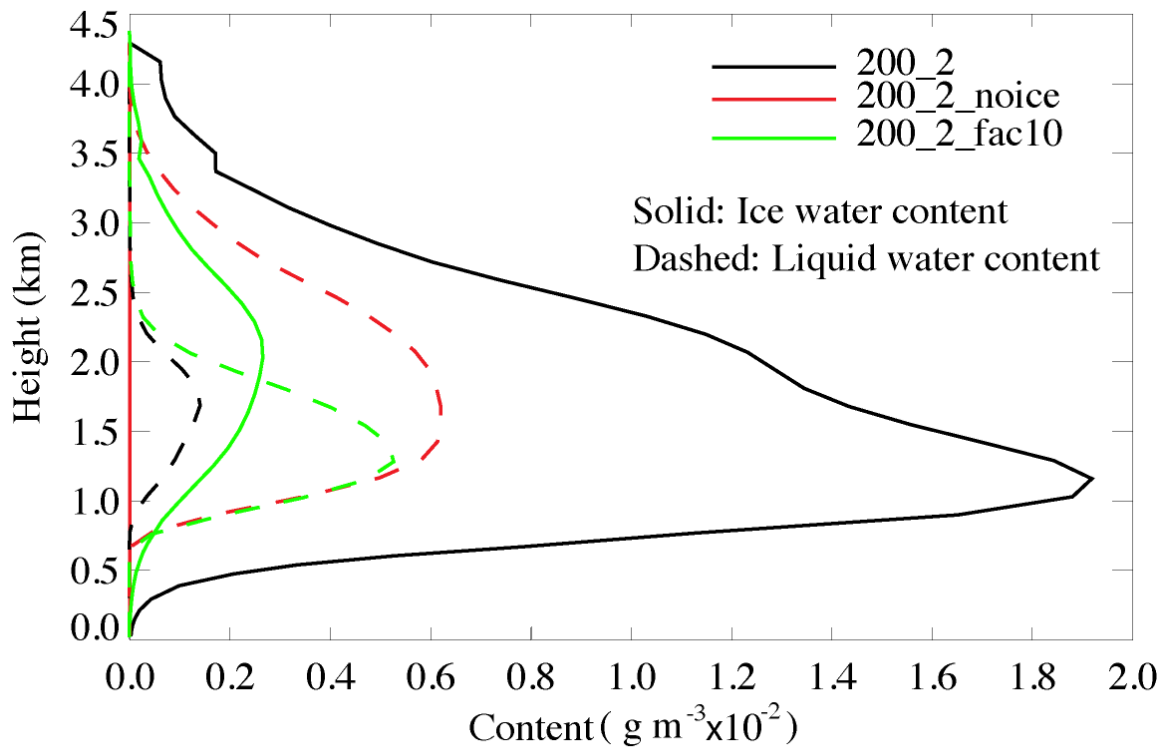
1273

1274

1275

1276

1277



1278

1279

**Figure 6**

1280

1281

1282

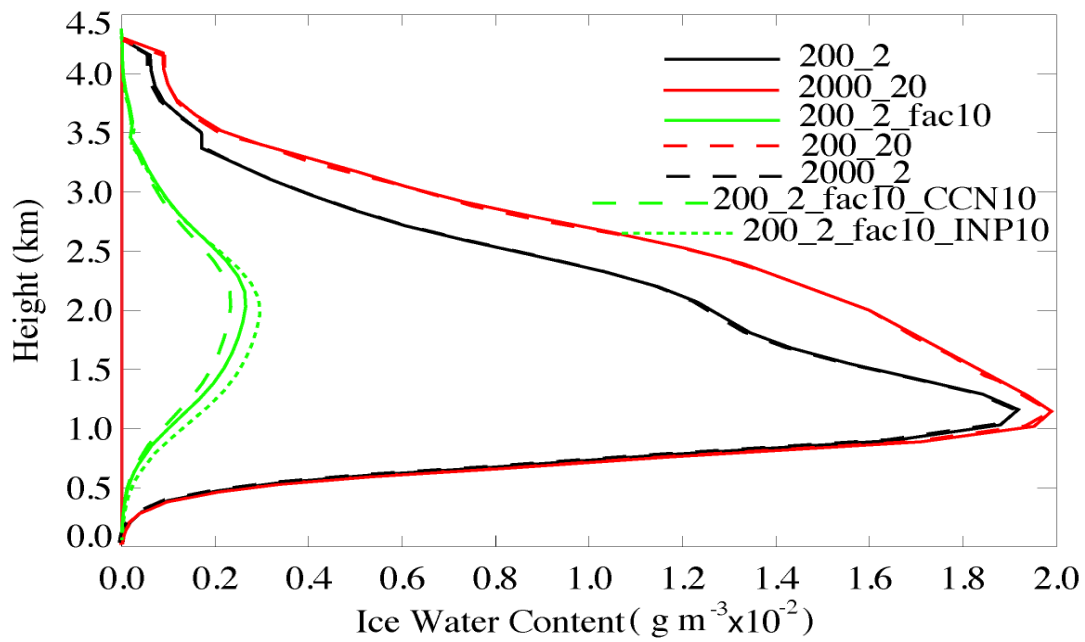
1283

1284

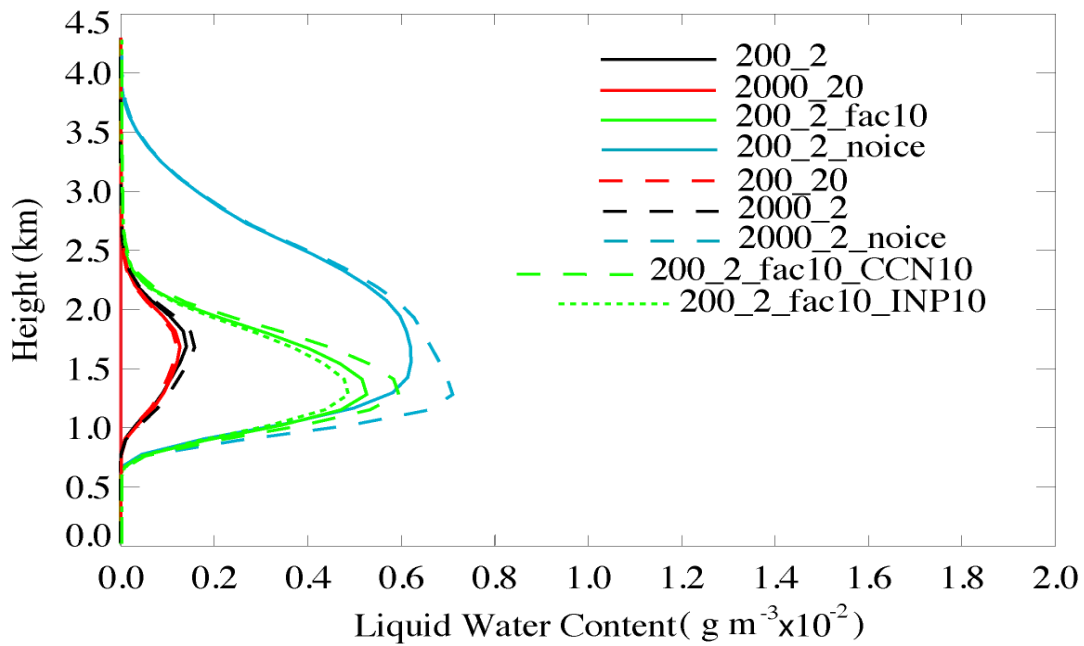
1285

1286

(a)



(b)



1287

1288

Figure 7